

CZECH UNIVERSITY OF LIFE SCIENCES PRAGUE

Faculty of Tropical AgriSciences



Czech University of Life Sciences Prague

**Faculty of Tropical
AgriSciences**

Genetic diversity of pangolins in Congo

MASTER'S THESIS

Prague 2020

Author: Bc. Iva Bernáthová

Chief supervisor: Mgr. Barbora Černá Bolfiková, PhD.

Second (specialist) supervisor: Doc. RNDr. Pavel Hulva, PhD.

Declaration

I hereby declare that I have done this thesis entitled Genetic diversity of pangolins in Congo independently, all texts in this thesis are original, and all the sources have been quoted and acknowledged by means of complete references and according to Citation rules of the FTA.

In Prague 15.5.2020

.....

Iva Bernáthová

Acknowledgements

First of all, I would like to thank Ing. Markéta Swiacká for the whole innovative idea regarding pangolins, for all the samples she has collected for this study and entrusted me, for her enthusiasm, optimism (that she kept despite the complicated situation in Congo) and assistance from the beginning to the end. I am very grateful to my theses supervisor, Mgr. Barbora Černá Bolfiková, PhD., who lead me and supported me throughout the whole work, for her patience and professional approach. Thanks also belong to my consultant, Doc. RNDr. Pavel Hulva, PhD., for his advicess and help with data interpretation.

I also appreciate the help from my lab colleague, Ing. Milena Jindřichová, with laboratory work. Ing. Silvie Neradilová and Mgr. Kristýna Elijášová helped me make the crazy software for data analysis work before I went crazy myself. I would like to thank Ing. Anna Kubátová for her help with the administrative work, namely obtaining the CITES permits. Lastly, thanks belong to Robert Masáre who helped me with designing a poster based in this study, for his support during writing the theses.

I am grateful for all the others I did not mention and who offered their support or assistance during creation of this theses.

This study was supported by Internal Grant Agency FTA grant No. 20195012, The Mohamed bin Zayed Species Conservation Fund and The Rufford Foundation.



Abstract

Pangolins (Pholidota) are a unique group of mammals from the superorder Laurasiatheria with many apomorphies mostly related to myrmecophagy including protective scales, trophic adaptations and expansion to semi-fossorial or arboreal niche. There are eight species of pangolins (four in Asia and four in Africa), all of them are listed on the IUCN Red List as threatened. Monitoring of pangolins using survey methods such as camera traps is difficult, since they are elusive, mostly nocturnal and live either in burrows or treetops. Molecular methods are therefore a great tool to study them. Our study focuses on two African species: the White-bellied Pangolin (*Phataginus tricupsis*) and the Giant Pangolin (*Smutsia gigantea*). We used 53 scales, 8 tissues and 3 buccal swabs collected from hunters and villagers in the area in Odzala-Kokoua National Park in Congo. The analyses were based on mitochondrial (control region) and nuclear (beta-fibrinogen, titin) markers. The study revealed high haplotype diversity and low nucleotide diversity in both species according to both mitochondrial and nuclear markers. The median-joining haplotype network for the control region revealed unique geographic lineage of *P. tricupsis* in Congo. Bayesian Skyline plots showed population expansion *P. tricupsis* which started 1.5 Mya, stable population course in *S. gigantea* and recent decline in both species. This is the first detailed population study of these species. Understanding the population biology of the studied populations may contribute to better conservation management and in the fight with illegal trade with these endangered animals.

Key words: illegal trade, pangolins, *Phataginus tricupsis*, phylogeny, population genetics, scales, *Smutsia gigantea*

Contents

1. Introduction and literature review	1
1.1. Origin and phylogeny of pangolins	1
1.2. Extant species and taxonomy	3
1.3. African pangolins.....	5
1.4. Asian pangolins	9
1.5. Wildlife forensics.....	11
1.5.1. Use in wildlife trafficking.....	11
1.5.2. Hunting and trade with pangolins	11
1.5.3. Uses of molecular methods in wildlife forensics	12
1.5.4. Tracking down the trafficking routes	13
1.6. Population genetics of pangolins	15
1.7. Pangolins in Congo	17
1.7.1. Species and their ecology	17
1.7.1.1. <i>Smutsia gigantea</i> (Giant ground pangolin).....	17
1.7.1.2. <i>Phataginus tetradactyla</i> (Black-bellied pangolin)..	18
1.7.1.3. <i>Phataginus tricupsis</i> (White-bellied pangolin).....	18
1.7.2. Conservation status and legislation	18
1.7.3. Local use and trade with pangolins	19
1.7.4. Pangolin populations in Congo	19
2. Aims of the Thesis	21
3. Material and methods	22
3.1. Samples and studied area.....	22
3.2. Laboratory analysis	24
3.2.1. DNA Extraction	24
3.2.2. Markers	24
3.2.3. Polymerase chain reaction (PCR)	25
3.2.4. Purification	26
3.2.5. Sequencing	26
3.3. Data processing and analysis.....	26
3.3.1. Mitochondrial data	26

3.3.2.	Nuclear data	28
4.	Results.....	30
4.1.	Mitochondrial data	30
4.2.	Nuclear data.....	34
5.	Discussion	37
5.1.	Population structure and dynamics	37
5.2.	Samples.....	40
5.3.	Use in pangolin conservation	41
6.	Conclusions	42
7.	References	43

List of tables

Table 1: Sequences of primers used in this study.	25
Table 2: PCR protocols used in this study.	25
Table 3: The summary statistics of <i>Phataginus tricupsis</i> (a) and <i>Smutsia gigantea</i> (b).	30
Table 4: The descriptive statistics of <i>Phataginus tricupsis</i> and <i>Smutsia gigantea</i> for beta-fibrinogen (FBG) and coding region of titin (TTN) genes.	35

List of figures

Figure 1: Complete phylogenetic tree of extant pangolins and their distribution..	3
Figure 2: Drawings, maps of distribution and IUCN Red list statuses of the eight extant species of pangolins.....	4
Figure 3: A map representing the potential geographical distribution of the six <i>Phataginus tricupsis</i> lineages (left) and phylogenetic tree of the six lineages (right).	6
Figure 4: Map of distribution of the six lineages of <i>Phataginus tricupsis</i> as delimited in the analysis of nuclear and mitochondrial markers.....	7
Figure 5: Phylogenetic tree of <i>Manis javanica</i> using single nucleotide polymorphisms (a) and the direction of introgression between lineages of <i>M. javanica</i> indicated by dashed arrows).	10
Figure 6: A map of possible trafficking routes..	14
Figure 7: Haplotype networks of <i>Smutsia temminckii</i> for cytochrome oxidase i(a), cytochrome b (b) and d-loop (c.) markers.	16
Figure 8: Scales of <i>Phataginus tricupsis</i> (a), <i>P. tetradactyla</i>	22
Figure 9: Map of geographic origin of samples used in this study.	23
Figure 10: Mismatch distribution analysis graphs for <i>Phataginus tricupsis</i> (a) and <i>Smutsia gigantea</i> (b).....	31
Figure 11: Bayesian skyline plot based on mitochondrial DNA of <i>Phataginus tricupsis</i> samples.....	31
Figure 12: Bayesian skyline plot based on mitochondrial DNA of <i>Smutsia gigantea</i> samples.....	32
Figure 13: Median-joining network of the mitochondrial control region haplotypes for 33 <i>Phataginus tricupsis</i> samples from congo and 105 GenBank <i>P. tricupsis</i> sequences..	33
Figure 14: Median-joining network of the mitochondrial control region haplotypes for 10 individuals of <i>Smutsia gigantea</i>	33
Figure 15: Landscape genetic shape interpolation analysis based on variation in control region of mitochondrial DNA for <i>Phataginus tricupsis</i>	34

Figure 16: Mismatch distribution analysis graphs for beta-fibrinogen (a) and coding region of titin (b) genes in *Phataginus tricupsis*. Pink line represents expected allele frequencies, blue line represents observed allele frequencies. 35

Figure 17: Median-joining haplotype network of the beta-fibrinogen gene for 23 *Phataginus tricupsis* samples from Congo and 95 GenBank *P. tricupsis* sequences.... 36

Figure 18: Median-joining haplotype network of the coding region of titin gene for 17 *Phataginus tricupsis* samples from congo and 98 GenBank *P. tricupsis* sequences. ... 36

List of the abbreviations used in the thesis

bp - base pair

BSP - Bayesian Skyline plot

CITES - Convention on International Trade in Endangered Species of
Wildlife Fauna and Flora

CA - Central Africa

COI - cytochrome oxidase I

CR - control region

cyt b - cytochrome b

DG - Dahomey Gap

ESS - effective sample size

ESU - Evolutionary Significant Unit

FBG - fibrinogen

Gab - Gabon

Gha - Ghana

IUCN - International Union for Conservation of Nature

kya - thousands years ago

LGB - Lower Guinean Block

MCMC -Markov chain Monte Carlo

mtDNA - mitochondrial DNA

Mya - million years ago

nDNA - nuclear DNA

PCR - polymerase chain reaction

SNM - Standard neutral model

SNP - single nucleotide polymorphism

STR - short tandem repeat

TTN - titin

UGB - Upper Guinean Block

US - United States of America

WAfr - Western Africa

WCA - Western-central Africa

1. Introduction and literature review

1.1. Origin and phylogeny of pangolins

Pangolins (Pholidota) probably arose on the Laurasian continents (Gaudin et al. 2009). The oldest fossil of pangolin (*Eomanis sp.*) was found in Messel deposits in Germany, thus Pholidota probably originated in Europe in the middle Eocene (45 Mya) and might have been distributed across Laurasian continents until the end of Eocene (Gaudin et al. 2006). Laurasian origin is supported by the fact that Pholidota are closely related to the Palaeanodonta and Carnivora, which both arose in North America (Gaudin et al. 2006, 2009; Yu et al. 2011).

Carnivora is the closest related group and a sister clade to Pholidota (Arnason et al. 2002; Gaudin et al. 2009; Gaubert et al. 2018; Kumar Prakash et al. 2018). Choo et al. (2016) suggested that Pholidota diverged from Carnivora approx. 56.8-67.1 Mya, yet only two pangolin species were included in the analysis.

Kumar Prakash et al. (2018) propose divergence time between Carnivora and Pholidota approx. 87.2 Mya based on analysis of mitochondrial DNA cytochrome b (cyt b) of seven extant species. Gaubert et al. (2018) suggests the split between the two groups occurred at a similar time, approx. 78.9 Mya. The divergence time is based on both mitochondrial and nuclear markers of all extant species and is therefore more accurate. The phylogenetic tree of extant pangolin species is given in Figure 1.

It is assumed that the ancestors of modern pangolins dispersed from Europe to Africa and subsequently to Southeast Asia (Gaudin et al. 2009; Du Toit et al. 2014). Pangolins probably migrated between Africa and Eurasia through so-called filter routes across Neo-Thetys. In the early Eocene, several islands and peninsulas connecting Afro-Arabian and Eurasian plates emerged and might have served for pangolin dispersal. Or alternatively they migrated later through the

Gomphotherium landbridge which occurred 16-20 Mya in the early Miocene between Eurasia and Arabic plate and allowed the exchange of mammals from Eurasia to Africa and vice versa (Sen 2013; Gaubert et al. 2018).

The African species seem to be more divergent than Asian species. This might be caused by the fact that the African lineage colonised its range some time before the Asian lineage and had more time to diversify (Gaudin et al. 2009). Pangolins remained restricted to tropics during Pleistocene climatic oscillations (Gaubert et al. 2018).

The extant pangolins are included in the family Manidae which comprise eight species (Gaubert et al. 2016) that range across two continents - sub-Saharan Africa and tropical and subtropical Asia. Asian species reach from India, Nepal and South China to Taiwan, Thailand, Myanmar, Indonesia and nearby Islands. African species' distribution range from Senegal, across the states along the Gulf of Guinea to central Africa, and South Africa in *S. temminckii* (MacDonald 2006).

According to both nuclear and mitochondrial DNA markers, African and Asian pangolins form two sister-groups (Zhang et al. 2015; Gaubert et al. 2018). This pattern is also supported by morphological data (Gaudin et al. 2009); most striking is the presence of hairs between scales in the Asian lineage (Challender et al. 2014).

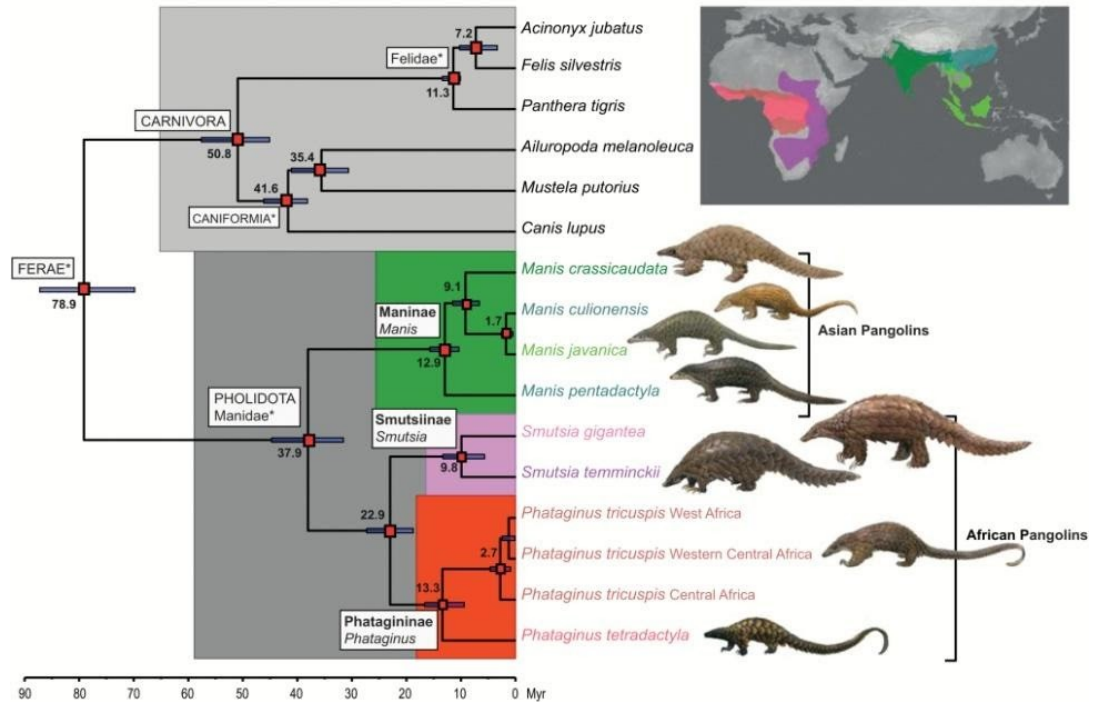


Figure 1: Complete phylogenetic tree of extant pangolins and their distribution. The numbers at nodes represent divergence times in millions years ago (adopted from Gaubert et al. (2018)).

1.2. Extant species and taxonomy

Pholidota consists of three families: Eomanidae, Patriomanidae and Manidae. All eight extant species of pangolins belong to the family Manidae, along with Plio-Pleistocene extinct species, the other two groups include only extinct species (Gaudin et al. 2009):

- *Manis crassicaudata* - the Indian pangolin
- *Manis pentadactyla* - the Chinese pangolin
- *Manis culionensis* - the Philippine pangolin
- *Manis javanica* - the Sunda pangolin
- *Manis tricuspis* - the White-bellied pangolin
- *Manis gigantea* - the Giant pangolin
- *Manis temminckii* - the Temminck's pangolin
- *Manis tetradactyla* - the Black-bellied pangolin

(‘Catalogue of Life’ (2020); see Figure 2)

Number of recognized genera has varied over time from one single genus *Manis* up to seven genera (Gaudin et al. 2006; Gaubert et al.

2016, 2020). Although, both extremes poorly describe phylogenetic relationships among the species.

Some authors propose the existence of three genera: *Smutsia* for Asian species, *Phataginus* for African tree species and *Smutsia* for African ground species (Gaubert et al. 2018; Kumar Prakash et al. 2018; Gaubert et al. 2020). Given the morphological differences and genetic distances among the three genera it seems that using three genera is more realistic than one single genus (Gaubert et al. 2018).

There is also discussion about the taxonomic status of geographic lineages of African species *P. tricuspis* observed by (Gaubert et al. 2016) based on mitochondrial and nuclear genes. The six identified lineages are currently considered Evolutionary Significant Units (ESUs), although some may even represent individual species. Yet further decisions would require more detailed study including more data.

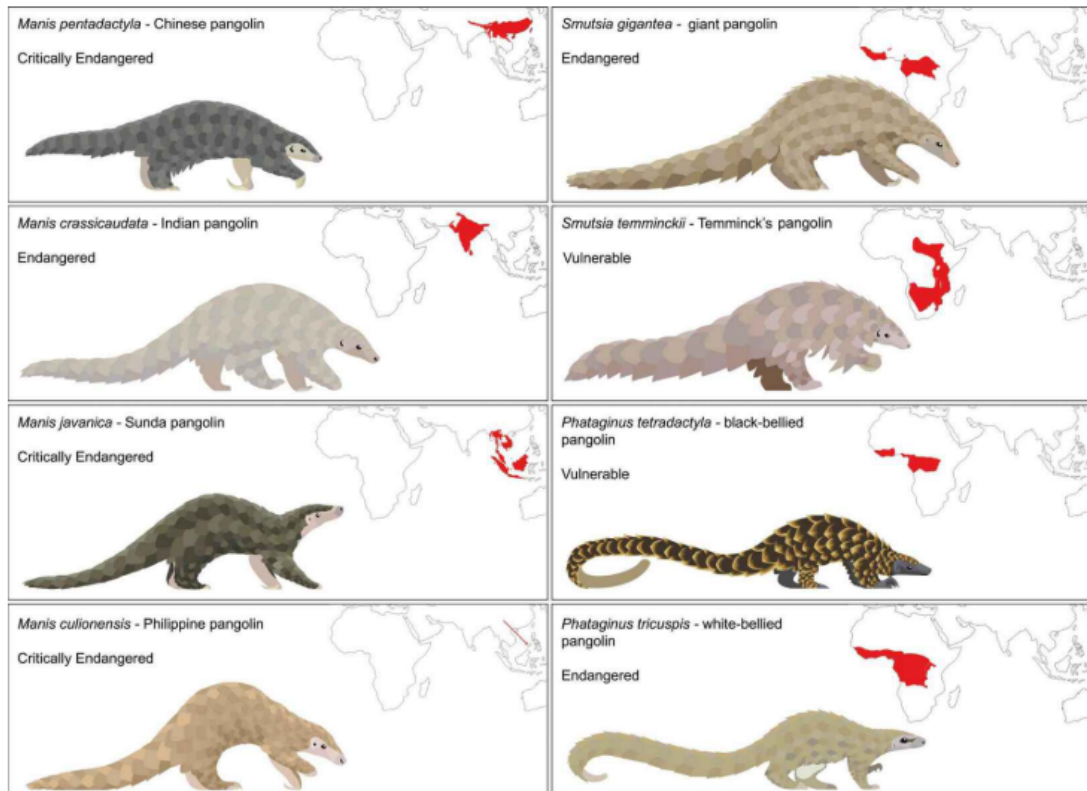


Figure 2: Drawings, maps of distribution and IUCN Red list statuses of the eight extant species of pangolins (adopted from Gaubert et al. (2020)).

1.3. African pangolins

Within the African group, the genera *Smutsia* (ground dwelling pangolins) and *Phataginus* (arboreal pangolins) are sister clades forming a monophyletic group (du Toit et al. 2017a; Gaubert et al. 2018). The arboreal species (genus *Phataginus*) split from the terrestrial pangolins (genus *Smutsia*) around 20.5 Mya according to mitochondrial data (Kumar Prakash et al. 2018). Gaubert et al. (2018) propose divergence time approx. 22.9 Mya according to mitochondrial and nuclear data (Figure 1).

The arboreal pangolins (*P. tricupsis* and *P. tetradactyla*) split from each other approx. 13.3 Mya (Gaubert et al. 2018). Both species have broadly sympatric distribution (i.e. in West and central Africa) and similar ecology; both are connected to forest or forest-savanna habitats (Ingram et al. 2019a; Pietersen et al. 2019b).

P. tricupsis has the best known phylogeographic history of all Pholidota thanks to a large-scale study conducted by Gaubert et al. (2016). They sampled the species across its range and used mitochondrial, nuclear and Y-borne genes for population assessment. Six distinct geographical lineages with non-overlapping ranges based on mtDNA were identified: western Africa (WAfr), Ghana (Gha), Dahomey Gap (DG), Western-central Africa (WCA), Gabon (Gab) and Central Africa (CA) (Figure 3). Nuclear DNA recovered three lineages: WCA, CA+Gab and WAfr+Gha+DG (Gaubert et al 2016, Figure 3). The differentiation of *P. tricupsis* started during Pleistocene around 2.1-2.7 Mya (Gaubert et al. 2018, see Figure 4).

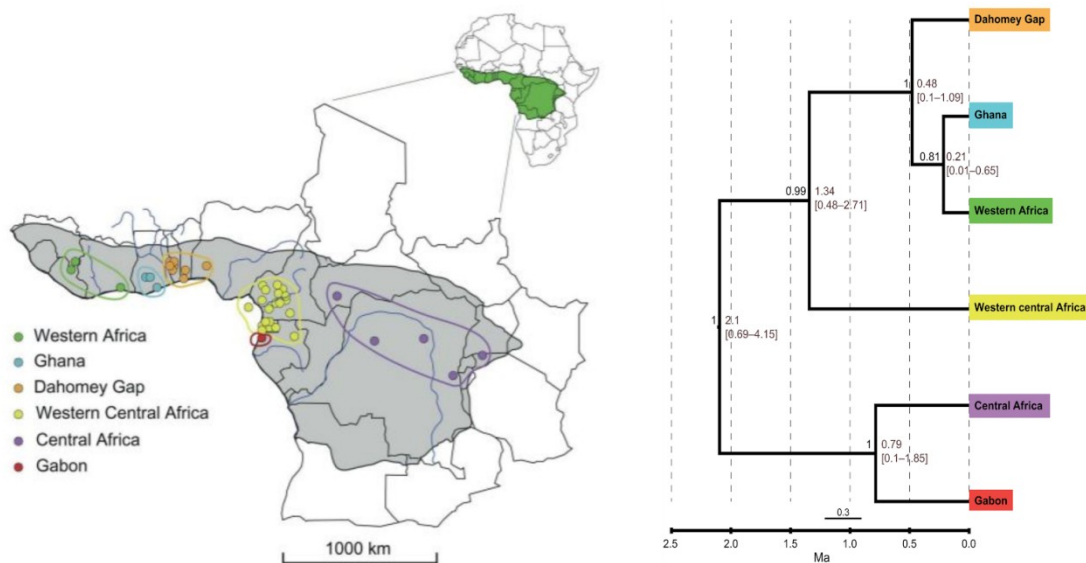


Figure 3: A map representing the potential geographical distribution of the six *Phataginus tricupsis* lineages (left) and phylogenetic tree of the six lineages (right) (adopted from Gaubert et al. (2016) (right) and Gaubert et al. (2020) (left)).

The diversification time may point to Pleistocene climatic oscillations. These oscillations are connected with the occurrence of glacial periods for which is typical increased aridity and drop of sea levels, and interglacial periods with warmer and more humid climate (Runge 2008).

In tropical Africa, glacial cycles caused repeated retraction of forest habitats to places where humid conditions were maintained even during arid periods. The forest-dwelling animals were therefore restricted to smaller patches of rainforest that played a role as refugia. The isolated populations could diversify and even give rise to new species (Nichol 1999; Runge 2008). Yet the role of these refugia in diversification of African rainforest organisms is still under debate (Anthony et al. 2007; Kirschel et al. 2011).

In *P. tricupsis*, the Pleistocene refugia might have driven the divergence of the six lineages, along with low dispersal potential of the species (Gaubert et al. 2016). The influence of rainforest refugia was confirmed in other African rainforest species such as gorillas (Anthony et al. 2007) or Misonne's pramys (Nicolas et al. 2011). The distribution

of lineages in W Africa, Ghana and coastal Lower Guinean Block (LGB) indeed fits the proposed refugia along coastal Lower and Upper Guinean Block (Gaubert et al. 2016).

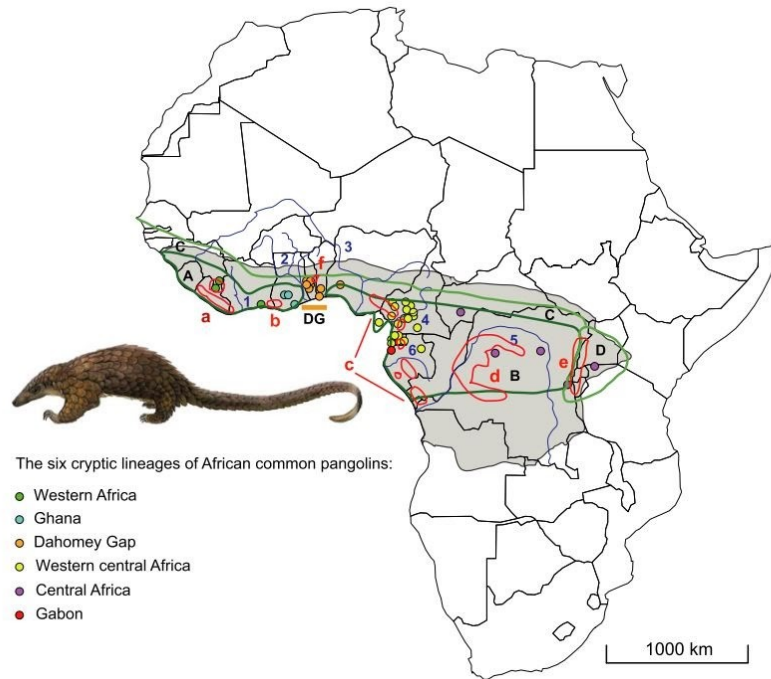


Figure 4: Map of distribution of the six lineages of *Phataginus tricupsis* as delimited in the analysis of nuclear and mitochondrial markers. Grey area corresponds to distribution of *P. tricupsis*. Green lines represent main biogeographical areas: A – Upper Guinean block; B – Lower Guinean block; C – Guinea–Congolia/Sudania transition zone; D – Guinea–Congolia/Zambezia transition zone. The main rivers crossing the Guineo–Congolian rainforest are given to illustrate potential biogeographic barriers: 1 – Sassandra; 2 – Volta; 3 – Niger; 4 – Sanaga; 5 – Congo; 6 – Ogooué. The Dahomey Gap (DG) is illustrated as a potential biogeographic barrier. Red contours represent rough delimitations of last glacial maximum rainforest refugia (adapted from Gaubert et al. (2016)).

Interestingly, the distribution of the six lineages of *P. tricupsis* does not match any of the major biogeographical zones, i.e. Upper and Lower Guinean Block, Guinea–Congolia/Sudania transition zone and Guinea–Congolia/Zambezia transition zone (see Figure 4). Western central African lineage shows split from other lineages included in Lower Guinean Block (LGB). This is a unique pattern among African rainforest animals since Western central Africa region is usually

included in the LGB biogeographic group, like in the case of woodpeckers (Fuchs & Bowie 2015), West African forest geckos (Leaché & Fujita 2010) or bristlebills (Huntley & Voelker 2016) where distribution of genetic lineages match with the two respective blocks of rainforest. This unique pattern in pangolins suggests a presence of a biogeographic barrier for pangolins that joined Gabon to eastern Cameroon and initiated the split of the WCA belonging to LGB and Gab lineage belonging to UGB (Hassanin et al. 2015; Gaubert et al. 2016).

The role of traditional barriers (e.g. large African rivers, see Figure 4) played a minor role in diversification of *P. tricupsis* (Gaubert et al. 2016). The area of Dahomey Gap (a broad savanna corridor delimited by Volta and Wémé rivers) was considered as a geographic barrier dividing UGB and LGB (Nichol 1999; Leaché & Fujita 2010; Fuchs & Bowie 2015, see Figure 4). However, the area of Dahomey gap was covered by forest or forest-savanna mosaic most of the Pleistocene period (Nichol 1999).

P. tricupsis can effectively adapt to more arid savanna or forest-savanna habitat (Akpona et al. 2008; Jansen et al. 2020). This ability may explain the presence of an endemic lineage in Dahomey Gap restricted between the Volta and the Niger rivers. The lineage probably arose from pangolins that migrated from West Africa and adapted to forest-savanna conditions of Dahomey gap. Therefore the Dahomey gap acted here rather as a refuge than a barrier (Gaubert et al. 2016).

Hassanin et al. (2015) revealed high nucleotide divergence between mitochondrial genes of the *P. tricupsis* specimen from Gabon and specimens from Ghana, Nigeria and Cameroon. This would also suggest the existence of a separate lineage in Gabon. Yet this analysis included the only sequence from one individual from Gabon without any other supporting data.

Exact geographical delimitation of the six lineages is still ambiguous due to low number of samples in certain areas (especially in Gabon where only one sample in both studies was included) or

uncertain geographical origin of the samples (Gaubert et al. 2016). The taxonomic status of the geographic lineages also remains unresolved (see Chapter 1.2; (Gaubert et al. 2016, 2018)).

The ground-dwelling pangolins (*S. gigantea* and *S. temminckii*) split from each other more recently, approx. 9.8 Mya (Gaubert et al. 2018). Both species are terrestrial and occupy savanna habitat, *S. gigantea* in western and western-central Africa, *S. temminckii* in south, south-east and north-east Africa (Nixon et al. 2019; Pietersen et al. 2019a).

1.4. Asian pangolins

According to mitochondrial and nuclear data, the divergence of the Asian group started approx. 12.9 Mya (Gaubert et al. 2018). Among the *Manis* genus (Asian pangolins), *M. pentadactyla* is the oldest species (Gaubert et al. 2018; Kumar Prakash et al. 2018, see Figure 1). *M. pentadactyla* is distributed across Himalaya mountains, south China, northern part of Malayan peninsula and nearby islands (Challender et al. 2019b).

M. crassicaudata emerged around 9.1 Mya according to mitochondrial and nuclear markers (Gaubert et al. 2018; Figure 1). *M. crassicaudata* is resident in the entire India, the distribution area reaches from Nepal to the north and to Pakistan to the west (Mahmood et al. 2019). The presence of a non-monophyletic lineage of *M. crassicaudata* in Sri Lanka might be a legacy of multiple dispersals of pangolins between Indochina mainland and nearby islands during the Pleistocene period of aridity (Gaubert & Antunes 2005).

M. javanica is distributed across Malay peninsula, Borneo, Java, Sumatra and adjacent islands (Challender et al. 2019a). Indochinese mainland population and island population diverged quite recently, approximately 0.61 Mya during middle Pleistocene. The migration between Malay peninsula and Indonesian islands occurred during glacial maxima when sea level dropped and forested land bridges

between mainland and islands were established that were used also by other species such as mouse deer (Mason et al. 2019).

In *M. javanica* three geographic lineages, probably from Borneo, Java and Singapore/Sumatra, were identified using single nucleotide polymorphisms (SNPs). A secondary gene flow occurs among the three lineages and is mainly driven by extensive trade with pangolins and their movement between regions (Nash et al. 2018), Figure 5). These genetic lineages may represent different conservation units or even species (Zhang et al. 2015; Luczon et al. 2016; Mwale et al. 2016). Given the wide distribution of the species, there may be additional cryptic diversity in *M. javanica* (Pietersen & Challender 2020).

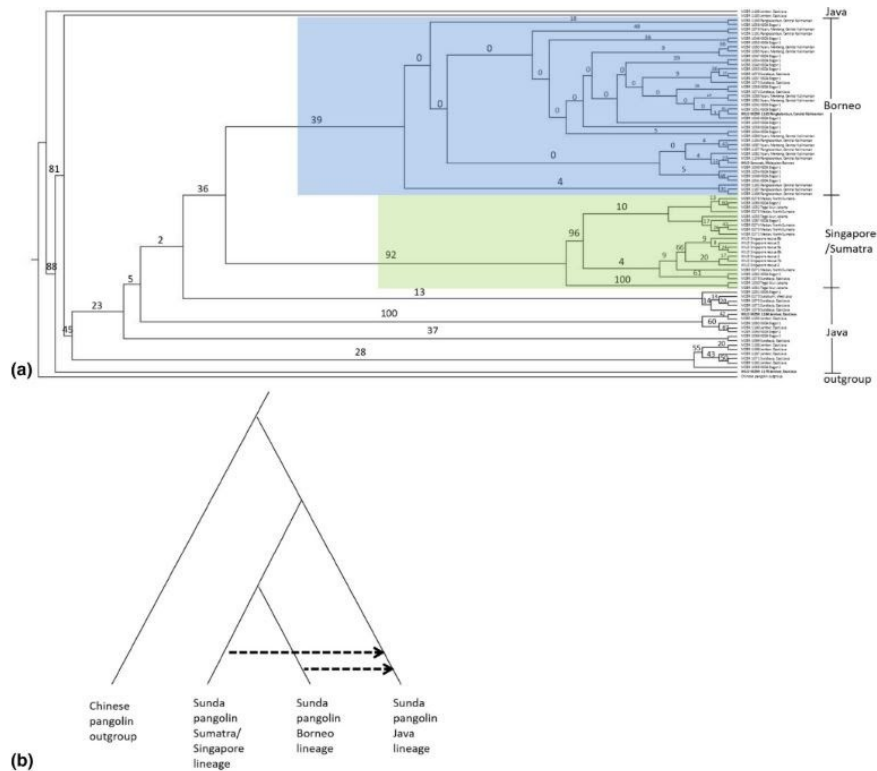


Figure 5: Phylogenetic tree of *Manis javanica* using single nucleotide polymorphisms (a) and the direction of introgression between lineages of *M. javanica* indicated by dashed arrows (adopted from Nash et al. (2018)).

The sister species of *M. javanica* is *M. culionensis* (Gaubert et al. 2018; Figure 1) that is restricted only to the Palawan islands (Schoppe et al. 2019). The ancestors (probably belonging to *M. javanica*) of *M. culionensis* migrated during Pleistocene glacial period from Borneo

through land bridges and afterwards remained isolated on Palawan islands (Luczon et al. 2016). Isolated individuals underwent rapid morphological changes driven by different habitats of newly occupied Palawan islands and evolved to a new species - *M. culionensis* (Gaubert & Antunes 2005).

1.5. Wildlife forensics

1.5.1. Use in wildlife trafficking

Molecular methods have proved to be useful in investigation of cases of illegal trade with wildlife products (Wasser et al. 2008) and in identification of species of seized animal's parts in the case of meat products (Kumar et al. 2014), skins and leathers (Jun et al. 2011) or monitoring illegal trade with ivory (Wasser et al. 2008). Molecular identification techniques (SNPs, microsatellites, DNA barcoding, etc.) are often transferred from conservation methods (Ogden et al. 2009).

Studies that call into account also phylogeography and population structure can help determine which populations or geographic units are the most affected by overexploitation. Knowledge about phylogeny, phylogeography and population genetic structure is necessary for application of molecular methods in wildlife forensics (Alacs et al. 2010).

1.5.2. Hunting and trade with pangolins

Pangolins are targeted globally and without discrimination among species (Mwale et al. 2016) Their hunting increased significantly over the last 42 years (Ingram et al. 2018). Pangolins are also being extensively trafficked from African countries to Asia. Hunting has therefore a major impact on pangolin populations (Challender et al. 2014; Ingram et al. 2019b).

There has been a shift in trade from Asian species of pangolins to African ones. Before the year 2000, the trade almost exclusively consisted of two Asian species, *M. javanica* and *M. pentadactyla*. Since

2001, there has been an increase in trade in African species and majority of the traded pangolins were identified as *P. tricupsis* or *S. gigantea* (Heinrich et al. 2016).

Scales and meat from Asian species are mostly used for medicinal purposes. These pangolins are therefore traded usually as body parts (Heinrich et al. 2016). African pangolins are trafficked from several African countries including Cameroon, Ghana, Nigeria and Republic of Congo to Asian markets (Ingram et al. 2019b), usually traded as whole animals (Heinrich et al. 2016). Part of hunted animals is sold on markets throughout Sub-Saharan Africa. Prices and demand for pangolins and their parts has increased on urban markets (Ingram et al. 2016).

The US also contributed to pangolin decline and was one of the top destinations of the pangolin skins which were imported mainly from Asian countries (Heinrich et al. 2017, 2019). Pangolin skins are still widely used there for leather products, although the trade with skins has declined over the last 20 years, partly because pangolin skin is being replaced by skins of other species or printed skin (Heinrich et al. 2019).

1.5.3. Uses of molecular methods in wildlife forensics

The specimen from wildlife forensic cases can be identified to species level using both nuclear DNA (nDNA) and mitochondrial DNA (mt DNA). Mitochondrial DNA markers are often favoured since it is easier to obtain sufficient amounts of DNA from non-invasive or degraded samples (Alacs et al. 2010).

Cytochrome oxidase I (COI) and cytochrome b (cyt b) are widely used universal mtDNA markers which can help identify species (Zhang et al. 2015; Mwale et al. 2016) of wildlife specimens or assign individuals to geographic areas (Zhang et al. 2015; Mwale et al. 2016; Kumar et al. 2016). In pangolins, d-loop was also used as a marker (Hsieh et al. 2011; Mwale et al. 2016; Gaubert et al. 2016). Geographic

origin can be identified only in the presence of known geographic structure over the species range (Rowe & Beebee 2008; Alacs et al. 2010).

Most commonly used nDNA markers are microsatellites (or short tandem repeats, STRs) and single nucleotide polymorphisms (SNPs) (Alacs et al. 2010). In combination with assignment tests, microsatellites and SNPs (Kumar et al. 2016; Nash et al. 2018) can provide information on geographic origin of wildlife specimens.

1.5.4. Tracking down the trafficking routes

Zhang et al. (2015) used COI marker and cytochrome b to determine the species identity of scales and carcasses confiscated in Hong Kong. The analysis identified that the majority of scales belong to *M. pentadactyla*. There were two samples that belonged to an unknown *Manis* species which formed a sister clade to *M. javanica*.

High numbers of haplotypes identified among the samples indicate that the pangolins are hunted from a vast area and then collected for processing and shipping at collection points (Zhang et al. 2015). Same pattern was observed in seized scales from Taiwan that were identified as *M. javanica* (Hsieh et al. 2011).

In another seizure from Hong Kong, which was believed to have been trafficked from Africa, were present both African species (*P. tricupsis*, *P. tetradactyla* and *S. gigantea*) and Asian species. Majority of the scales of Asian origin were assigned to *M. javanica*, yet there were also present scales whose identity could not be verified. They belonged either to an unknown species or species that was not included in the analysis. The exact geographic origin was not determined due to lack of reference material (Mwale et al. 2016).

Kumar et al. (2016) figured out that seized scales from different parts of India (based on mtDNA cyt b and 16S rRNA) were identified as *M. pentadactyla* which means that *M. pentadactyla* is poached across its range and its scales distributed on markets across the entire India.

DNA barcoding was used to identify species identity in two cases of seized pangolins in the Philippines. The confiscated pangolins were suspected to be *M. culionensis*. COI analysis revealed that the seizures contained bodies of *M. culionensis* and also *M. javanica*. *M. javanica* is non-native in the Philippines, poachers therefore collected the pangolins outside the Philippines. *M. javanica* samples from one of the seizures formed two groups in phylogenetic analysis and thus poached at least two different locations (Luczon et al. 2016).

Nash et al. (2018) identified three genetic lineages in heavily traded *M. javanica* using SNPs. These genetic lineages are restricted to Borneo, Java and Singapore/Sumatra. The presence of *M. javanica* lineages help as well reveal the course of illegal trade in Southeast Asia (see Figure 6). Illegal trade and movement of animals over larger distances caused by humans can jeopardize the geographic lineages and it is therefore important to monitor the trade with pangolins and adapt conservation activities to protect and manage each lineage separately.

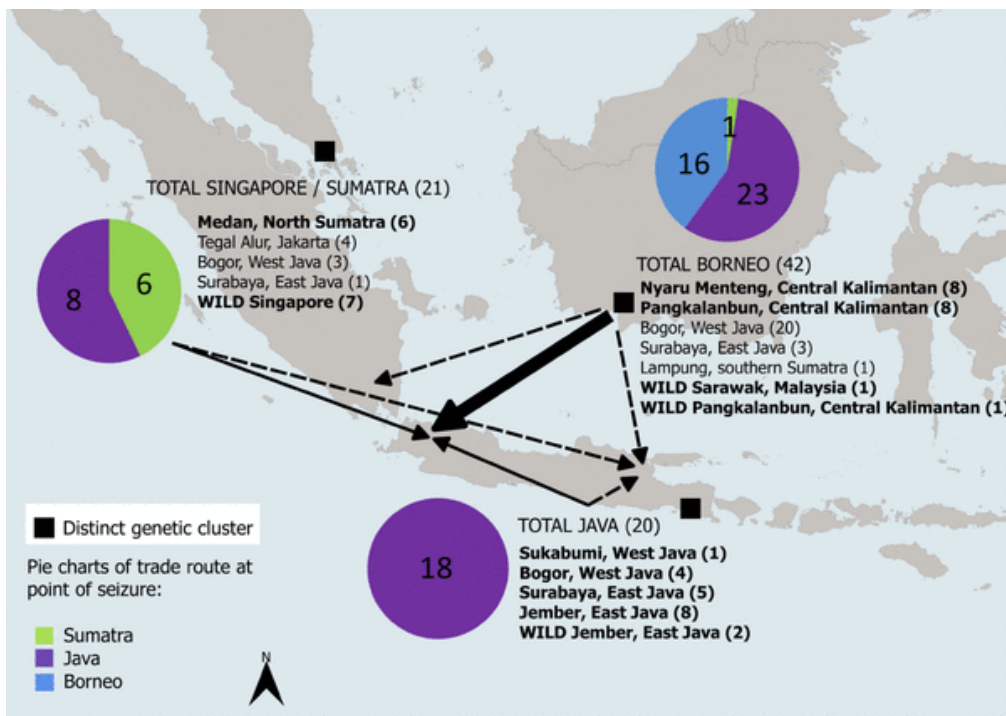


Figure 6: A map of possible trafficking routes. Arrows indicate the direction of trade, the arrow size are proportional to trade volume, dashed arrows indicate less volume traded (adopted from Nash et al. 2018).

1.6. Population genetics of pangolins

There are only few studies describing population parameters and structure of pangolin species. Larger population level research has not been conducted in *P. tetradactyla*, *S. gigantea* or Asian species (Pietersen & Challender 2020).

First intraspecies markers for pangolins were developed by Luo et al. (2007). Microsatellite markers included 34 loci and revealed relatively high heterozygosity in *M. javanica* and *M. pentadactyla* and a possible sub-structuring of its population. This study contained only 24 and 12 individuals. Vãn Thao et al. (2006), on the contrary, reported low genetic diversity in the population of *M. javanica* in samples from Vietnamese rescue center and Taiwanese markets in a study based on mitochondrial control region.

De Beer (2013) used the same microsatellite markers in *S. temminckii*. He described that the population of *S. temminckii* has significantly lower observed heterozygosity ($H_o=0.416$) than *M. javanica* ($H_o=0.634$; Luo et al. 2007) and that there is a certain level of admixture within the population (De Beer 2013). Results might have been influenced by the small sample size or small number of investigated loci.

Another study using 11 microsatellite markers in African species of pangolins showed high observed heterozygosity in *S. gigantea* ($H_o=0.514$), *S. temminckii* ($H_o=0.559$) and *P. tricupsis* ($H_o=0.541$) in comparison to *P. tetradactyla* ($H_o=0.241$) (du Toit et al. 2020). Different values of heterozygosity may be due to different numbers of markers or different samples sizes in both studies.

The most comprehensive population study was conducted by du Toit (2014) who used mitochondrial markers (cytochrome oxidase I (COI), cytochrome b (cyt b) and d-loop to assess population genetic structure in *S. temminckii* across South Africa. The observed haplotype diversity was quite high (ranging between 0.788-0.934). Number of

identified haplotypes were 18 for the COI, 12 for cyt b and 16 for the d-loop. Only a few individuals represented private haplotypes (Figure 7).

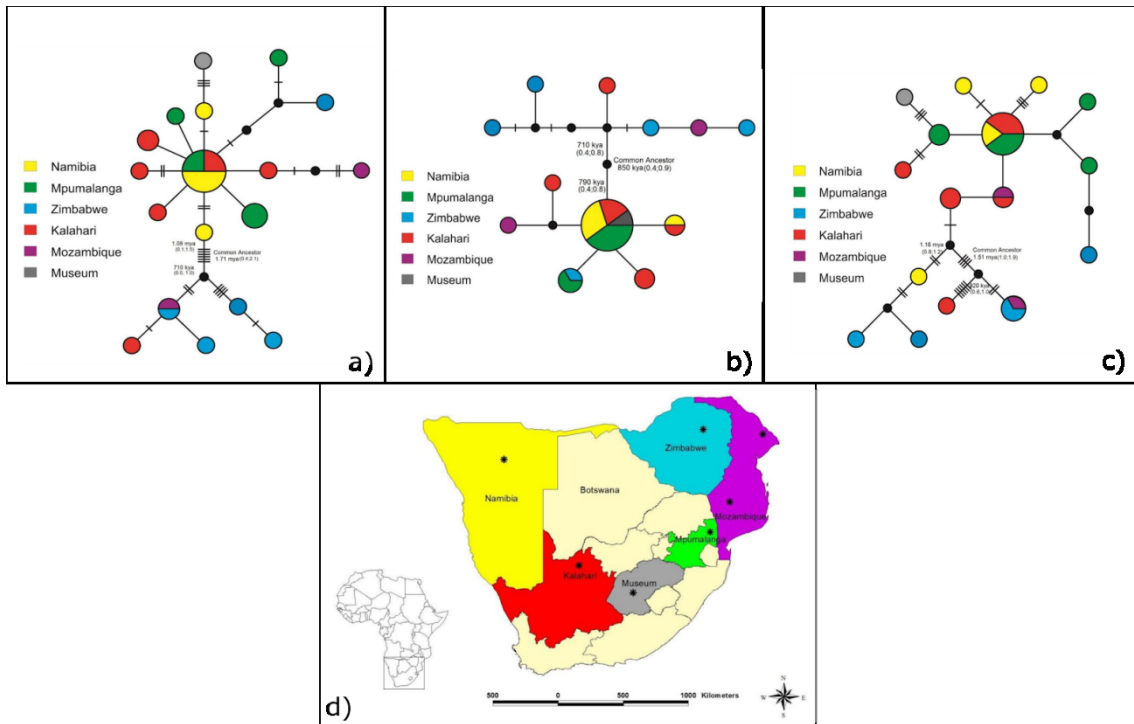


Figure 7: Haplotype networks of *Smutsia temminckii* for cytochrome oxidase I(a), cytochrome b (b) and d-loop (c.) markers. Each circle represents different haplotype, sizes are proportional to the number of individuals that share the haplotype, black points represent hypothetical haplotypes, lines between haplotypes represent number of mutations that haplotype underwent. Numbers next to the nodes represent molecular dates when two groups split from each other. Map (d) shows sampling regions of *S. temminckii*, colours of each correspond with colour in haplotype networks (modified from du Toit 2014).

Analysis showed the existence of two geographical units, one occurring in Zimbabwe/Mozambique and another restricted to Kalahari/Namibia/Mpumalanga with divergence time around 2.94-1.27 Mya. The observed differentiation was high between the two units but low between populations in each unit. The same pattern was observed in all three markers (du Toit 2014).

The highest genetic distances were observed between Mpumalanga and Mozambique and between Mpumalanga and

Zimbabwe. This pattern also supports the existence of two separated units (du Toit 2014)

The divergence between the two main lineages might have been caused by formation of arid, unsuitable habitat (so called Mega Kalahari Sand Sea) between the two areas during the Pleistocene period of aridity. Alternatively, the barrier was formed more recently and was human-induced. The low level of differentiation between the populations in each unit suggests that there is still some level of gene flow between the units (du Toit 2014). However, no nuclear markers were used in this study and the sample size was quite low therefore the results should be considered as preliminary.

1.7. Pangolins in Congo

1.7.1. Species and their ecology

There are three pangolin species occurring in the area of the Republic of Congo. All three species differ by morphology (i. e. size, number of scales, shape of scales), habitat preferences and ecology (Challender et al. 2014).

1.7.1.1. *Smutsia gigantea* (Giant ground pangolin)

S. gigantea is the largest and heaviest pangolin species in Congo and also in the world. *S. gigantea* inhabits a wide variety of habitats (primary and secondary forests, swamp forest and wooded savannah) (Hoffmann et al. 2020).

Its body is covered in more than 17 rows of overlapping protective scales. Powerful forelimbs have large claws which the animals use for destroying termite hills or digging it's burrows. However, they can also use disused burrows of another species (Kingdon et al. 2013; Hoffmann et al. 2020). Day activity depends on prey presence and season, it is more diurnal in dry season, more nocturnal in rainy season (Hoffmann et al. 2020).

1.7.1.2. *Phataginus tetradactyla* (Black-bellied pangolin)

P. tetradactyla is a small arboreal species occurring in West and Central Africa, with Congo Basin being the eastern limit of its range. The species has a long prehensile tail, black face and underside (Gudehus et al. 2020).

Its head and whole body except under parts are covered in 10-13 rows of sharply pointed scales which are distinguishable by dark colour with pale margins and edges (Kingdon et al. 2013; Gudehus et al. 2020). *P. tetradactyla* is often confused with *P. tricupsis*, despite significant differences in skin and scale colour or body size (Swiacká 2019; Gudehus et al. 2020).

P. tetradactyla shows more diurnal activity than other species, is predominantly solitary and prey mostly on ants (Gudehus et al. 2020).

1.7.1.3. *Phataginus tricupsis* (White-bellied pangolin)

P. tricupsis is the most common pangolin species in Congo and also the most widely sold species on bushmeat markets. In suitable habitats (including man-made habitats such as plantations), white-bellied pangolins live in relatively high densities (Akpona et al. 2008; Jansen et al. 2020). Their bodies are covered in small brownish-grey, three-cusped scales (Kingdon et al. 2013; Jansen et al. 2020).

P. tricupsis live predominantly in tree tops but they feed mostly on the ground. Individuals are territorial, males' territories partly overlap with females' territories (Jansen et al. 2020). *P. tricupsis* prey on ants and termites and they act as the insect regulators in the ecosystems. They also affect soil processes by excavating burrows in the ground (Challender et al. 2014; Jansen et al. 2020).

1.7.2. Conservation status and legislation

The three pangolin species are listed as threatened on the IUCN Red List with decreasing populations (IUCN 2020). After last assessment in 2019, *P. tetradactyla* has status Vulnerable (Ingram et al.

2019a) and *P. tricupsis* and *S. gigantea* are assessed as Endangered (Nixon et al. 2019; Pietersen et al. 2019b).

Since 1995, all eight species has been included in Appendix II of CITES (Species+ 2020). In 2016, the four African species were moved to Appendix I of CITES due to overexploitation and decreasing population numbers, as well as all Asian species (CITES 2017). The entire group Pholidota is also listed Annex A of EU Wildlife Trade Regulations (Publication Office of the European Union 2019).

1.7.3. Local use and trade with pangolins

The local communities in Congo are well informed about pangolins and their conservation status and legislation. Despite this, the hunting activities still continue and the hunting pressure on pangolins is significant. Pangolin meat and scales are sold at local bushmeat markets, mainly for medicinal purposes (Swiacká 2019).

There were four reported seizures in Congo between 2015 and 2018. The seizures included several kilograms of scales and whole pangolin bodies from different pangolin species (Ingram et al. 2019b). Last year (i.e. 2019), there were several large seizures of tens of tons of pangolin scales destined to Asia and part of the scales probably originated also in Congo (Ichu 2019). So it seems that pangolin hunting and illegal trade exceed the local markets.

1.7.4. Pangolin populations in Congo

There is very little data about the pangolin populations in Congo since their behaviour and ecology make them difficult to monitor and survey. Proxy data seem to be the most cost-effective methods in pangolin monitoring (Willcox et al. 2019). Such proxy data can be obtained using local-scale data from hunters and villagers. The use of proxy data can help evaluate hunting pressure on wildlife populations and estimate population abundance in hunting-sensitive species such

as pangolins in areas where other methods are too costly or cannot be used (Ingram et al. 2018; Willcox et al. 2019).

Local-scale data were used by Swiacká (2019) to assess populations of the three pangolin species in Congo. According to respondents' answers, the most sighted species was the white-bellied pangolin (*P. tricupsis*); this species was also the most frequent one at local bushmeat markets. Since *P. tricupsis* might be confused with similar arboreal sympatric species *P. tetradactyla*, the actual number of sighted individuals might differ in both species.

In some areas (namely south-western part of Odzala-Kokoua National Park), people reported *S. gigantea* as the most frequently encountered. Population of *S. gigantea* might be more abundant in particular parts of Congo due to more suitable habitat (i.e. forest-savanna mosaic). Law enforcement is more applied in *S. gigantea* than in both arboreal species so it might also help their populations (Swiacká 2019).

Interestingly, villagers denoted the pangolin population in Congo as increasing, most likely because they saw pangolins or tracks of pangolins during hunting (Swiacká 2019). However, pangolin populations are thought to be decreasing because of hunting pressure, and also habitat destruction (Challender & Hywood 2012; Challender et al. 2014; Ingram et al. 2018).

2. Aims of the Thesis

The aim of the study is to assess and compare the genetic diversity, demographic parameters and phylogeographic history of two pangolin species (*P. tricupsis* and *S. gigantea*) occurring in the Odzala-Kokoua NP in Congo.

3. Material and methods

3.1. Samples and studied area

Samples used in this study were collected from villagers and hunters in the area of the Odzala-Kokoua National Park and its surroundings in the north of Congo, and in several villages and bushmeat markets in the south of Congo in May and June 2018. List of sampled villages is given in the Appendix 1.

Majority of the samples come from killed animals observed at the markets or in the villages except one buccal swab which was taken from a living individual. The samples were given by dwellers and merchants voluntarily and they did not get paid for the samples since this was an ethical restriction. Date and time of collection, GPS coordinates, species (determined by size, colour and morphology of the scale, see Figure 8) and amount of each sample were noted.

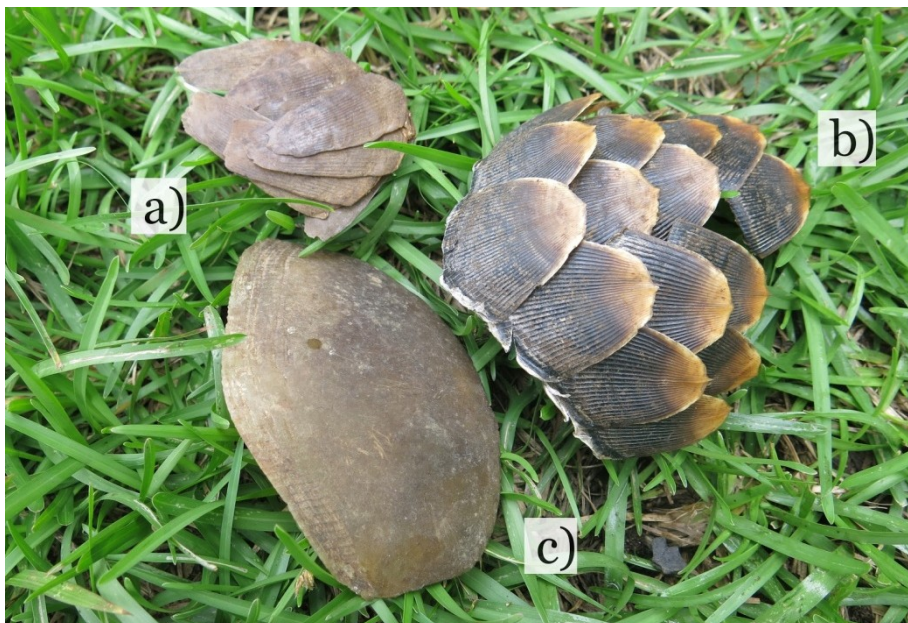


Figure 8: Scales of *Phataginus tricupsis* (a), *P. tetradactyla* (b; not included in this study) and *Smutsia gigantea* (c). Author: Markéta Swiacká

The samples included 53 scales, 8 tissues (pieces of tongue or oesophagus) and 3 buccal swabs. Tissues and swabs were fixed in 96% ethanol; scales were dried and placed in plastic bags with silica gel. After the transportation to the laboratory, all samples were stored in a refrigerator at -20°C. A map (Figure 9) of geographic origin of sampled individuals was created in ArcMap 10.7.1 (ESRI 2014).

All necessary research permits and documentation were obtained. We have obtained export (Nos. CG1125877, CG1125874 and CG1125875) and import (No. 18CZ028796) CITES permits and veterinary permit (No. 3009329) for all samples used in this study.

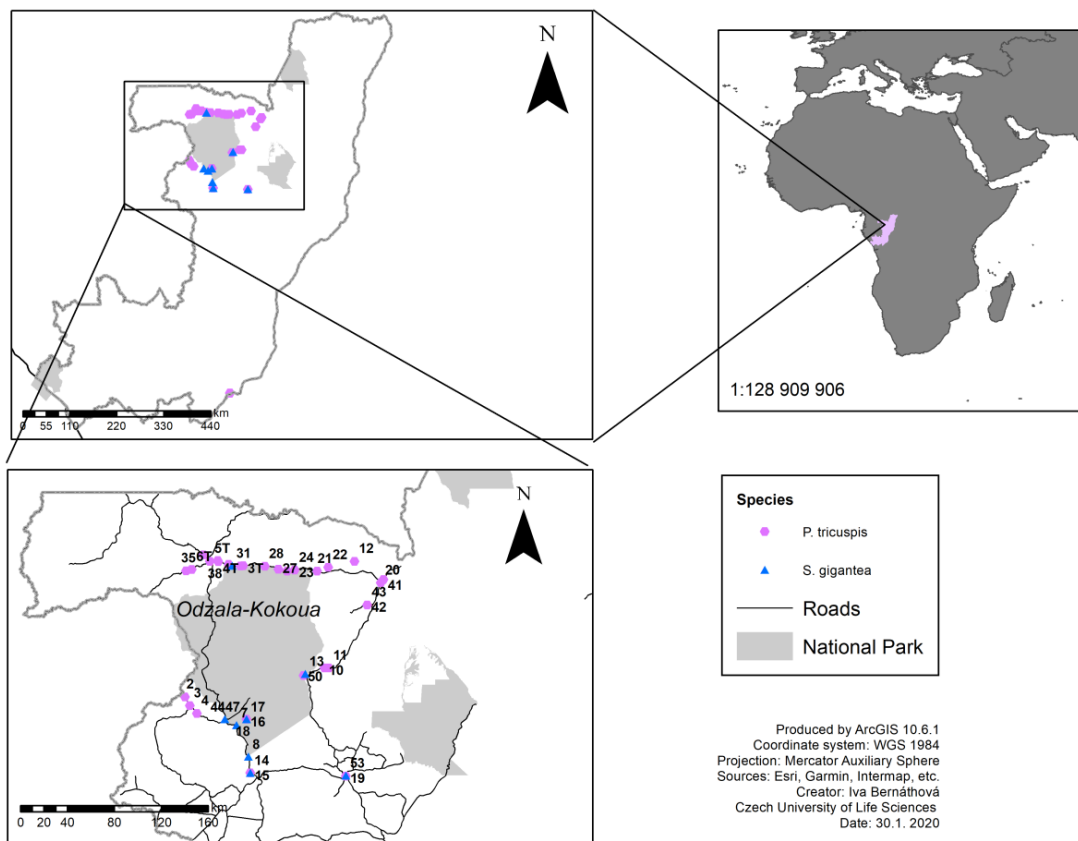


Figure 9: Map of geographic origin of samples used in this study.

3.2. Laboratory analysis

3.2.1. DNA Extraction

Genomic DNA from scales and tissues was extracted using commercial DNeasy Blood&Tissue Kit (Qiagen) following the manufacturer's protocol. In the case of scales, 30 μ l of dithiotreitol (DTT) was added during tissue lysis to enhance the lysis of keratin. In the last step, the DNA was eluted by 2 \times 30 μ l of Buffer AE (Elution Buffer).

Genomic DNA from buccal swabs was extracted using Presto Buccal Swab gDNA Extraction Kit (GenAid) and eluted by 50 μ l of Elution Buffer.

Concentration of extracted genomic DNA of each sample was measured with the spectrophotometer Nanodrop 2000 (ThermoScientific). The extracted DNA was stored in a refrigerator at -20°C.

3.2.2. Markers

For the purposes of this study, we have chosen two types of markers. Hypervariable mitochondrial DNA (mtDNA) control region (CR) which is suitable for population genetic studies because it has high mutation rate and is therefore highly variable (especially D-loop).

Mitochondrial DNA is maternally inherited, so we are able to trace the maternal lineage. We presumed that DNA extracted from the scales will be fragmented, resulting in a low number of intact copies, mainly due to unfavourable environmental conditions or heat processing done by villagers before consuming. Therefore we have decided to amplify shorter fragments of the left hypervariable domain of control region rather than control region in its whole length (i.e. around 1260 bp).

We have chosen two primer pairs that were designed to produce two amplicons of mtDNA CR with overlapping ends. Amplicons named DL and B1 of mtDNA CR were amplified using primer pairs

PNG_DloopF-PNG_DloopR (du Toit et al. 2017b) and L15997uni-panDH15972 (Hsieh et al. 2011), respectively.

For phylogenetic structure reconstruction, two nDNA markers were chosen. Nuclear markers show less intraspecific variability than mtDNA markers, yet still enough variability (especially non-coding introns) so they should allow phylogenetic tree reconstructions and tracing both maternal and paternal lineage.

Intron 7 of beta-fibrinogen (FBG) gene was amplified using primer pair FBG7PangF-FBG7PangR (Gaubert et al. 2016) and fragments of titin (TTN) using primer pair ManTTN4272R-ManTTN3571F (Gaubert et al. 2016). All primer sequences and fragment lengths are listed in Table 1.

Table 1: Sequences of primers used in this study.

name	primer sequence (5'→3')
PNG_DloopF	CGT TCC TCT TAA ATA AGA CAT CTC G
PNG_DloopR	TCT TGC TTT TGG GGT TTG AC
ManTTN4272-R	ACC GGT ATA GGC TGG AGG TT
ManTTN3571-F	CCC GTG GAA ACT GTT GAT GC
FBG7PangF	CCT CAT GCT TCA GCA AAA CA
FBG7PangR	GCT CTG GCC CCT CTA CTC TT
L15997uni	AGC CCC CAA AGC TGA TAT TCT
panDH15972	AGG GCA TGA CAC CAC AGT TAT G

3.2.3. Polymerase chain reaction (PCR)

Polymerase chain reaction (PCR) was performed in T100 Thermal cycler (BIO-RAD) in 25 µl of reaction mixture containing 12.5 µl PPP Mater Mix, 8.5 µl RNase-free water, 1 µl of each 10µM primer and 2 µl of genomic DNA. The PCR protocols are given in Table 2.

The efficiency of PCR reactions was determined by gel electrophoresis on 1% agarose gel.

Table 2: PCR protocols used in this study.

step	temperature	time (min)	fragment
1.	95°C	10	all
2.	95°C	0:30	all

3.	56°C	0:40	FBG, B1, DL
	52°C	0:40	TTN
4.	72°C	0:45	TTN, FBG, B1
	72°C	0:40	DL
5.	go to step 2., 40 ×		
6.	72°C	5:00	all
7.	12°C	for ever	all

3.2.4. Purification

Successfully amplified fragments were purified using Invisorb Fragment CleanUp Kit (Invitek Molecular GMBH) and eluted with 20 µl of Elution Buffer. PCR product concentration was measured with the spectrophotometer Nanodrop 2000.

3.2.5. Sequencing

Sequences of successfully amplified DNA fragments were produced by Sanger method with one primer of each primer pair (PNG_DloopR or PNG_DloopF for DL amplicon, L15997uni or panDH15972 for B1 amplicon, FBG7PangF or FBG7PanR for FBG and ManTTN4272R or ManTTN3571F for TTN) in either one or both direction depending on sequence quality. Sequencing was conducted in the service laboratory at Faculty of Science, Charles University.

3.3. Data processing and analysis

3.3.1. Mitochondrial data

MtDNA control region sequences were successfully obtained from 33 individuals of *P. tricupsis* and 10 individuals of *S. gigantea*. The rest of the samples was excluded due to unsuccessful PCR amplification or low quality of sequences.

Sequences were edited and aligned in Geneious 10.2.6 (www.geneious.com) software. In the case of mtDNA control region, a

consensus sequence from the two amplicons of CR was generated for each individual.

The population structure and dynamics can be determined by several methods. For basic assessment of population variability, the following parameters were calculated in DnaSp6 (Rozas et al. 2017): number of haplotypes (N_h), haplotype diversity (H_d), nucleotide diversity (p_i), raggedness statistics (r).

Mismatch distribution analysis comparing expected and observed frequencies of pairwise distances was calculated also in DnaSP6 (Rozas et al. 2017). Unimodal distribution indicates population expansion, multimodal distribution indicates population with mutation-drift equilibrium.

The neutrality test allow to distinguish population expansion and genetic hitchhiking. For both species, DnaSP6 (Rozas et al. 2017) was used to calculate neutrality tests - Tajima's D (D), R^2 , Fu's F_s (F_s). The statistical significance of the neutrality was tested against Standard Neutral Model (SNM).

Negative values of Tajima's D and Fu's F_s indicate population expansion or negative selection. Positive values indicate population decline or balanced selection, typical for populations after bottlenecks.

Population size changes in time for each species were assessed using coalescent-based Bayesian skyline plots (BSPs) calculated in BEAST 1.8.4 (Drummond & Rambaut 2007). In both *P. tricupsis* and *S. gigantea*, a strict molecular clock and HKY+gamma substitution model was used. The substitution model was determined by jModelTest (Guindon & Gascuel 2003; Darriba et al. 2012) in both species. For clock calibration, *P. tetradactyla* was used as an outgroup for *P. tricupsis* and *S. temminckii* as an outgroup for *S. gigantea*. Divergence times between respective species were adopted from Gaubert et al. (2018), i.e. 13.3 Mya in *P. tricupsis*/*P. tetradactyla* and 9.8 Mya in *S. gigantea*/*S. temminckii*. The MCMC procedure was run once for each species with 10,000,000 iterations, the genealogy and parameters of the

model were stored every 1,000 iterations, burn-in period was set to 1,000,000. The effective sample sizes (ESSs) for calculated parameters were checked in Tracer 1.7.1 (Rambaut et al. 2018) to be >200. Results of the analysis were then visualized in Tracer 1.7.1.

Median-joining (Bandelt et al. 1999) haplotype networks for each species visualizing relationships among individual haplotypes were created in Network 10.0 (www.fluxus-engineering.com) software. In *P. tricupsis*, the sequences were compared also with GenBank data (Accession numbers KX642071–KX642171, MG196296–MG196298, MF536683).

In the case of *S. gigantea*, we haven't found enough data in GeneBank, therefore the haplotype network was calculated only using our dataset.

Genetic Landscape Shape Analysis for *P. tricupsis*, showing relationship between genetic and geographic distances was interpolated by Alleles in Space 1.0 (AIS) software (Miller 2005) . A graph from the interpolated distances was created where peaks should represent samples with high genetic distances. *S. gigantea* was excluded also from the Genetic Landscape Shape Analysis due to low number of samples.

3.3.2. Nuclear data

Sequences of beta-fibrinogen (FBG) gene were successfully obtained from 23 individuals of *P. tricupsis* and 10 individuals of *S. gigantea*. Sequences of coding region of titin (TTN) gene were obtained from 17 individuals of *P. tricupsis* and 4 individuals of *S. gigantea*. The rest of the samples was excluded from the analysis due to unsuccessful PCR amplification or low quality of sequences.

Sequences were edited and aligned in Geneious 10.2.6 (www.geneious.com) software.

The haplotypes were phased using Phase 2.1.1 (Stephens et al. 2001; Stephens & Scheet 2005) software, the procedure was run separately for each species.

The following parameters were calculated in DnaSp6 (Rozas et al. 2017): number of haplotypes (N_h), haplotype diversity (H_d) and nucleotide diversity (p_i).

Median-joining (Bandelt et al. 1999) haplotype networks of beta-fibrinogen and titin genes for *P. tricupsis* visualizing relationships among individual haplotypes were created in Network 10.0 (www.fluxus-engineering.com) software. The sequences of individuals from Congo were compared also with GenBank data (Accession numbers KX642173-KX642267 and KX642269-KX642364; JN632925 for FBG and TTN sequences, respectively).

4. Results

4.1. Mitochondrial data

We have found 23 and 7 haplotypes in datasets of *P. tricupsis* and *S. gigantea*, respectively. Haplotype diversity (H_d) was quite high in both species and the nucleotide diversity (pi) low, indicating recent population expansion. Population neutrality tests reached negative values in both species, also indicating recent population growth, yet were significant only in *P. tricupsis* (see Table 3).

Table 3: The summary statistics of *Phataginus tricupsis* (a) and *Smutsia gigantea* (b). Number of individuals (N), number of haplotypes (N_h), haplotype diversity (H_d), nucleotide diversity (pi), Tajima's D (D), R^2 , Fu's F_s (F_s) and raggedness statistics (r) are given for each species and whole dataset.

* $p < 0.05$

*** $p < 0.001$

Species	n	N_h	H_d	pi	D	R^2	F_s	r
<i>P.</i> <i>tricupsis</i>	33	23	0.9678	0.0068	-1.6992*	0.0589*	-12.5741***	0.0065***
<i>S.</i> <i>gigantea</i>	10	7	0.9111	0.0072	-0.1275	0.1751	-0.3676	0.1274

Mismatch distribution analysis shows unimodal distribution in *P. tricupsis* (Figure 10 (a)) which again indicates population expansion. Mismatch distribution in *S. gigantea* shows multimodal distribution (Figure 10 (b)), indicating equilibrium between mutation and drift.

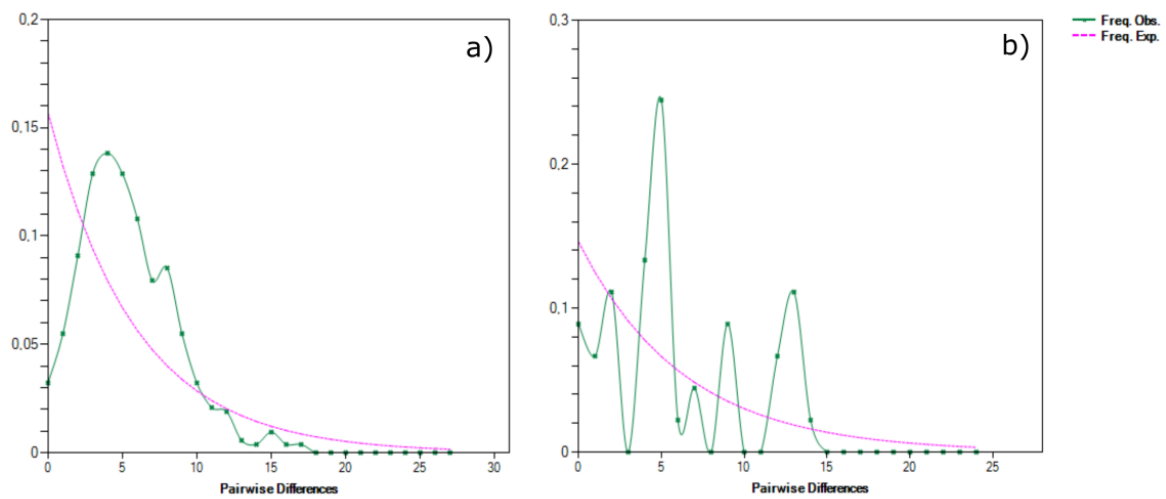


Figure 10: Mismatch distribution analysis graphs for *Phataginus tricupsis* (a) and *Smutsia gigantea* (b). Pink line represents expected allele frequencies, green line represents observed allele frequencies.

The Bayesian skyline plot in *P. tricupsis* (Figure 11) indicated a stable effective population size with a rapid growth approximately 1.5 Mya and signs of recent decrease. In *S. gigantea*, the BSP (Figure 12) shows stable effective population size with a decrease that started around 500 kya.

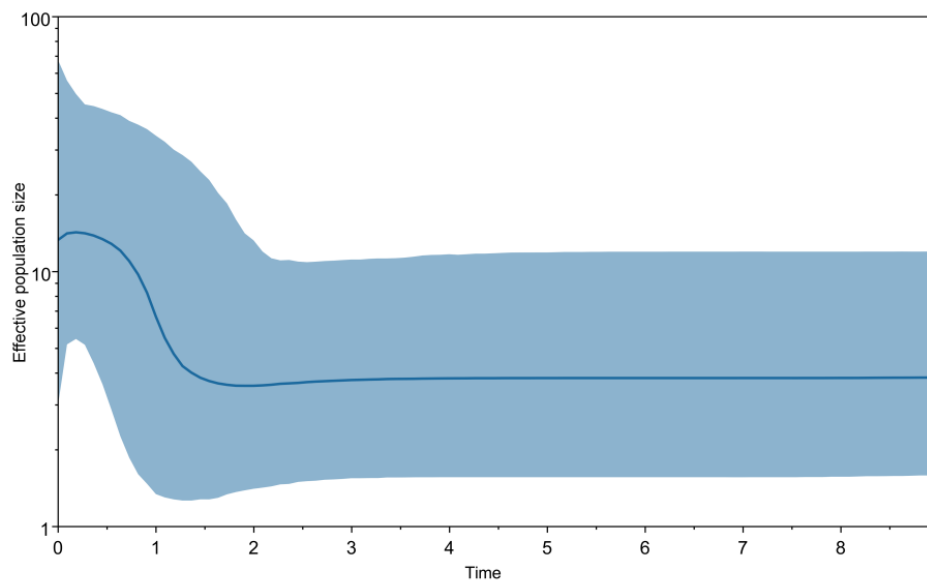


Figure 11: Bayesian skyline plot based on mitochondrial DNA of *Phataginus tricupsis* samples. The X axis represents the time in million years before present (0 represents present), the Y axis represents effective population size (N_e), the black line shows median of N_e , blue areas indicate 95% confidence interval.

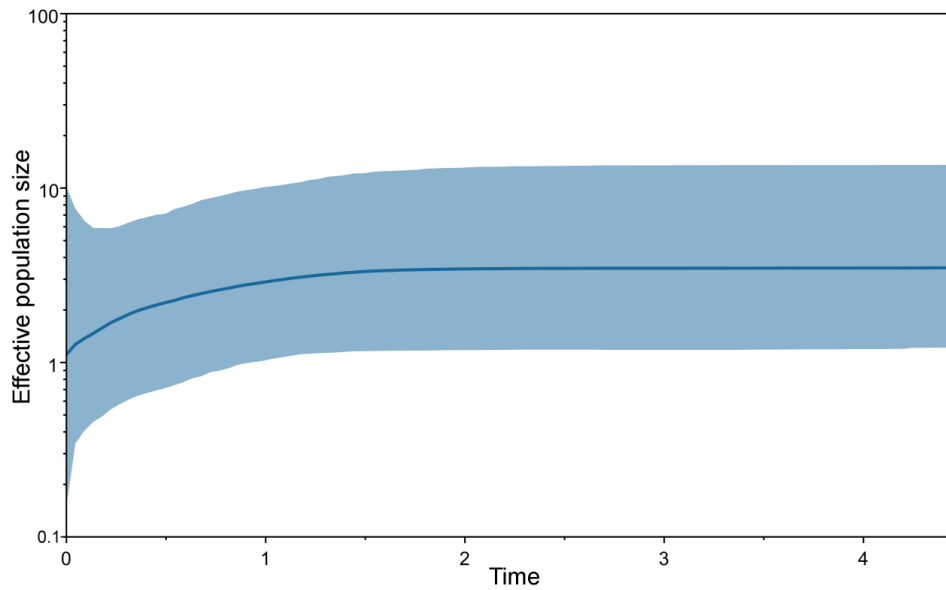


Figure 12: Bayesian skyline plot based on mitochondrial DNA of *Smutsia gigantea* samples. The X axis represents the time in million years (0 represents present), the Y axis represents a correlate of the effective population size (N_e), the black line shows median of N_e , blue areas indicate 95% confidence interval.

Median-joining haplotype network of *P. tricupsis* (Chyba! Nenalezen zdroj odkazů.) is quite complex. The majority of individuals from Congo do not share haplotypes with individuals from other areas. One exception is a sample no. 23 from Nakoaka in North Congo that shares haplotype with samples from Yaunde market and Bipindi in Cameroon. Haplotypes from Congo connect Western-central and Central-African haplotypes.

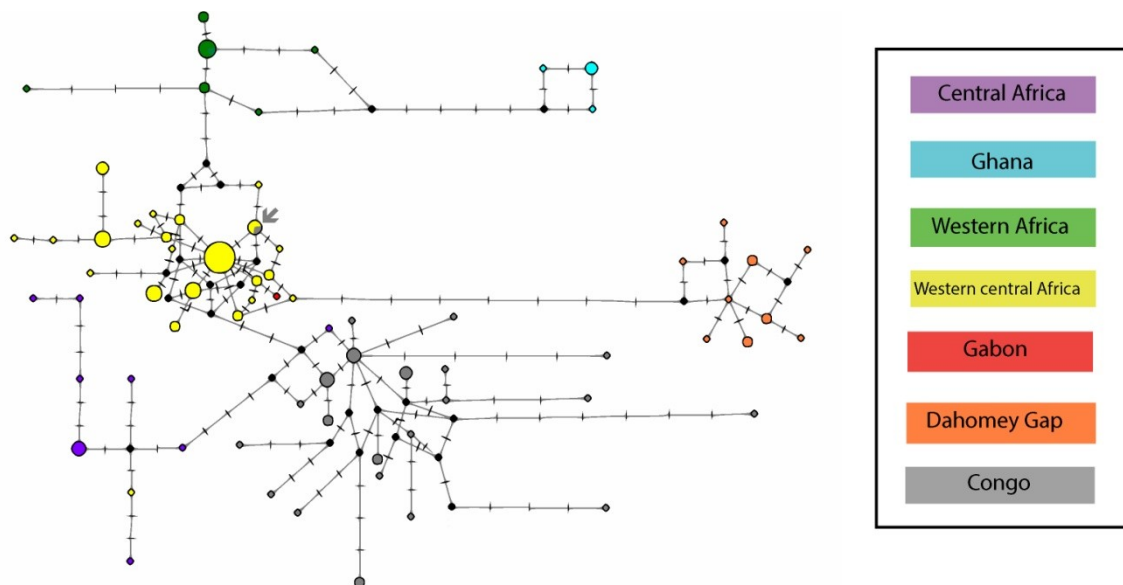


Figure 13: Median-joining network of the mitochondrial control region haplotypes for 33 *Phataginus tricupsis* samples from Congo and 105 GenBank *P. tricupsis* sequences. Haplotypes are represented by circles, which are proportional to haplotype frequency. The hypothesized haplotypes are represented by black dots. Colour codes are used according to six phylogeographic lineages showed in the phylogenetic tree (Gaubert *et al.* 2016). Lines between haplotypes represent nucleotide changes. Grey arrow indicates individual from Nakoaka.

Median-joining network for *S. gigantea* (Figure 14) is less complex due to lower number of samples.

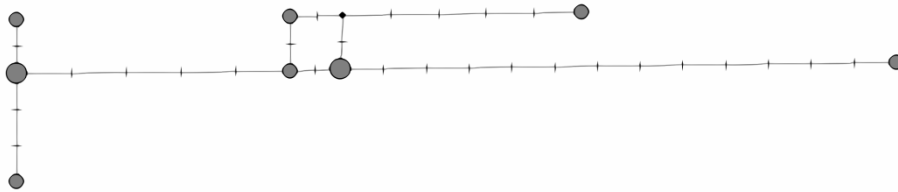


Figure 14: Median-joining network of the mitochondrial control region haplotypes for 10 individuals of *Smutsia gigantea*. Haplotypes are represented by dots, which are proportional to haplotype frequency. The hypothesized haplotypes are represented by black dots. Lines between haplotypes represent nucleotide changes.

Genetic Landscape Shape Analysis of *P. tricupsis* (Figure 15) population detected low genetic distances among samples in Odzala-Kokoua NP, represented by valleys in the graph. On the contrary, high genetic distances were observed among samples from the south of Congo represented by peaks in the graph.

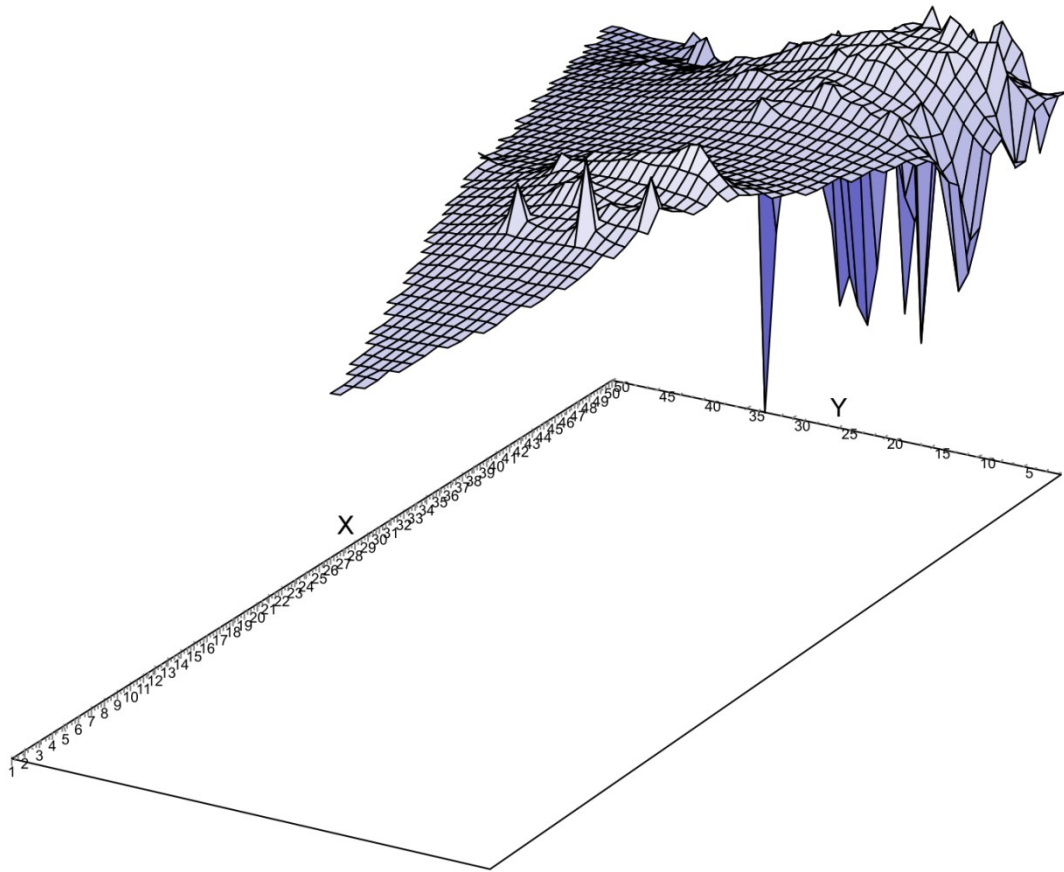


Figure 15: Landscape genetic shape interpolation analysis based on variation in control region of mitochondrial DNA for *Phataginus tricupsis*. X and Y axes reflect the geographic coordinates in the study area (latitude and longitude, respectively), Z axis represents the average genetic distances between analysed individuals.

4.2. Nuclear data

We have found 13 and 14 haplotypes in the beta-fibrinogen gene in datasets of *P. tricupsis* and *S. gigantea*, respectively and 17 and 1 haplotypes in the coding region of titin gene datasets of *P. tricupsis* and *S. gigantea*, respectively (Table 4). Haplotype diversity (H_d) was high for beta-fibrinogen in both species and the nucleotide diversity (p_i) low, like in the case of mitochondrial data. Same pattern was observed in the titin gene in *P. tricupsis*. Descriptive statistics were not calculated for titin gene in *S. gigantea* due to low number of sequences and low number of haplotypes found in the dataset.

Table 4: The descriptive statistics of *Phataginus tricupsis* and *Smutsia gigantea* for beta-fibrinogen (FBG) and coding region of titin (TTN) genes. Number of individuals (n), number of haplotypes (N_h), haplotype diversity (H_d), nucleotide diversity (π) are given for each species and whole dataset.

Species	n	N_h	H_d	π
FBG				
<i>P. tricupsis</i>	23	13	0.784	0.00589
<i>S. gigantea</i>	10	14	0.852	0.00129
TTN				
<i>P. tricupsis</i>	17	4	0.528	0.00184

Mismatch distribution analysis for *P. tricupsis* (Figure 16) shows unimodal distribution in both nuclear genes which indicates population expansion.

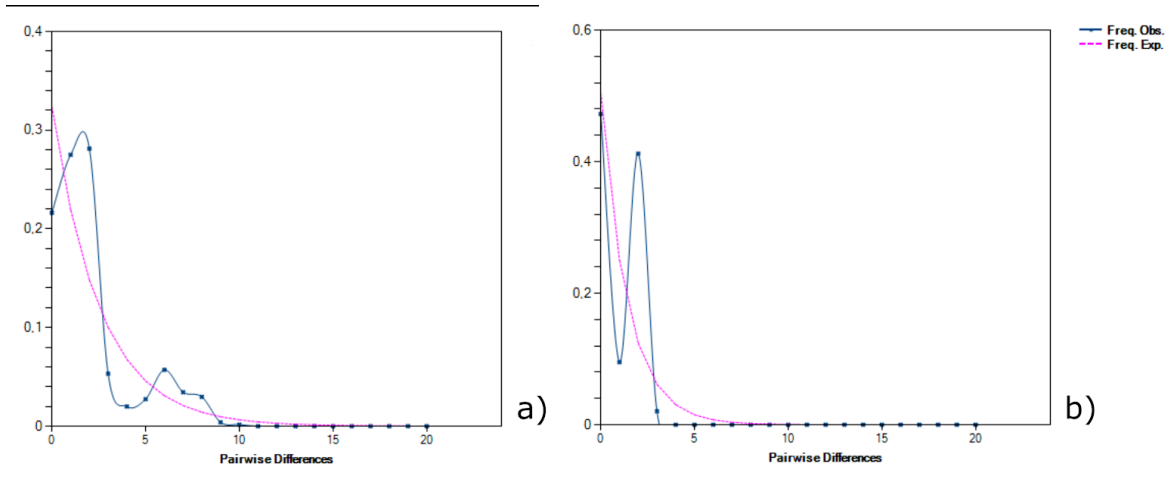


Figure 16: Mismatch distribution analysis graphs for beta-fibrinogen (a) and coding region of titin (b) genes in *Phataginus tricupsis*. Pink line represents expected allele frequencies, blue line represents observed allele frequencies.

Median-joining haplotype network of beta-fibrinogen gene for *P. tricupsis* (Figure 17) indicates 12 haplotypes. Majority of the individuals from Congo form discrete haplotypes, 9 share haplotype with samples originating in Central Africa and 3 samples share haplotype with individuals from Western Africa/Dahomey Gap.

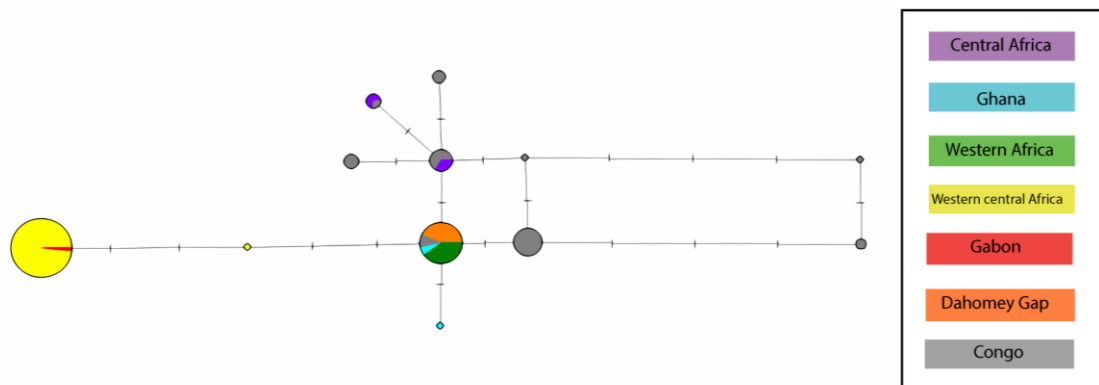


Figure 17: Median-joining haplotype network of the beta-fibrinogen gene for 23 *Phataginus tricupsis* samples from Congo and 95 GenBank *P. tricupsis* sequences.. Haplotypes are represented by circles, which are proportional to haplotype frequency. Colour codes are used according to six phylogeographic lineages in the phylogenetic tree of Gaubert et al. (2016) in Figure 3. Lines between haplotypes represent nucleotide changes.

Median-joining haplotype network of titin gene for *P. tricupsis* (Figure 18) indicates 6 haplotypes. The individuals from Congo share haplotype with samples originating in Central Africa, Western-central Africa/Gabon and Western Africa/Dahomey Gap.

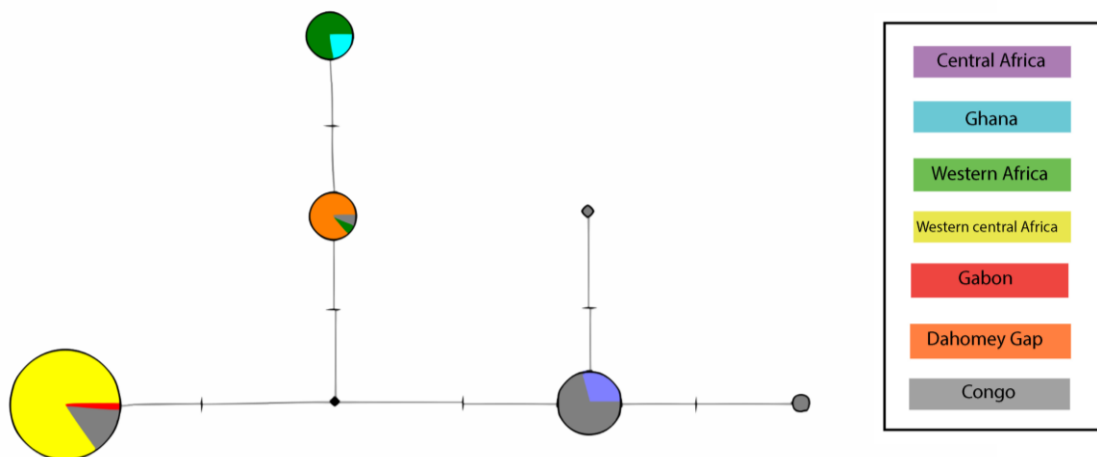


Figure 18: Median-joining haplotype network of the coding region of titin gene for 17 *Phataginus tricupsis* samples from Congo and 98 GenBank *P. tricupsis* sequences. Haplotypes are represented by circles, which are proportional to haplotype frequency. Colour codes are used according to six phylogeographic lineages in the phylogenetic tree of Gaubert et al. (2016) in Figure 3. Lines between haplotypes represent nucleotide changes.

5. Discussion

5.1. Population structure and dynamics

According to mitochondrial DNA control region, both species show high haplotype diversity (0.9678 and 0.9111 in *P. tricupsis* and *S. gigantea*, respectively) and low nucleotide diversity (0.0068 and 0.0072 in *P. tricupsis* and *S. gigantea*, respectively). Quite high haplotype diversity indicated also nuclear genes; in *P. tricupsis* showed beta-fibrinogen (0.784) more diversity than titin (0.528).

Similar levels of haplotype diversity (0.920, 0.980, 0.524, 0.554 for cyt b, control region, beta-fibrinogen and titin, respectively) and also nucleotide diversity (0.038, 0.025, 0.006, 0.002 for cyt b, control region, beta fibrinogen and titin, respectively) in *P. tricupsis* were observed by Gaubert et al. (2016). Du Toit (2014) detected high haplotype diversity using mitochondrial genes in populations of the ground-dwelling *S. gigantea* in South Africa .

High levels of haplotype diversity can be connected with low mobility and high territoriality of pangolins (Akpona et al. 2008; Khwaja et al. 2019; Jansen et al. 2020) which allow the individuals to diversify even in small areas. Low nucleotide diversity in combination with high haplotype diversity point to a recent population expansion.

Bayesian skyline plots indicate stable effective population sizes in both species. In *P. tricupsis*, there was a quite recent growth of effective population size around 1.5 Mya during Pleistocene. Population expansion is supported also by Mismatch distribution analysis for all three genes (CR, FBG, TTN) and neutrality tests. Interestingly, the expansion started during the period of increased aridity in Africa and decreased forest cover (deMenocal 2004). This fact is unusual in a species which is fixed to forest habitat and large trees (Akpona et al. 2008; Jansen et al. 2020). It seems that *P. tricupsis* is, to some extent, capable of adaptation to various conditions and is not fixed solely to

rainforest habitats, possibly also the expansion signal is driven by recent lineages showing affinity to drier and open-canopy forests. This ability is supported by the quite high occurrence rate of *P. tricuspis* in anthropogenic habitats nowadays (Challender et al. 2014; Willcox et al. 2019; Jansen et al. 2020). The expansion pattern could also be region specific, as illustrated by star-like phylogeny in mitochondrial haplogroup from western and central Africa, contrasting with larger average haplotype distances in other haplogroups.

Mismatch distribution for CR in *S. gigantea* indicates a rather stable population. The Bayesian Skyline plot for CR supports a stable effective population size in *S. gigantea* with a recent decline (500 kya) which could have been caused by habitat changes. The decline is probably currently accelerated by growing hunting pressure. However, the hypervariable mtDNA markers may not reflect the very recent (last 20-30 years) and fast population changes caused by anthropogenic factors. Therefore we cannot estimate the actual population trend in both species.

Median-joining haplotype network for control region in *P. tricuspis* indicates that individuals from Congo form a separated lineage which is connected with both Western-central and Central African lineage described by Gaubert et al. (2016), except for a sample from Nakoaka which shares haplotype with individuals from Cameroon and belong therefore to the Western-central African lineage. The existence of separate lineage in Congo indicates that there might be more cryptic diversity within the population of *P. tricuspis* across its range.

Still the distribution of the lineage from Congo detected in this study and the lineages from Western central Africa and Gabon remain unresolved since sampling does not cover the entire potential area of distribution of the geographic lineages.

The median-joining haplotype network for beta-fibrinogen gene in *P. tricuspis* revealed 11 haplotypes, five of which were discrete to individuals from Congo, several individuals shared haplotype with

individuals from Central Africa and, quite interestingly, with individuals from Western Africa/Ghana/Dahomey Gap.

The median-joining haplotype network for titin gene in *P. tricupsis* indicated only 6 haplotypes, two were discrete to the individuals from Congo. Haplotypes were shared with Central African and Western-central African/Gabon lineages. The haplotype networks show the pangolins from Congo share haplotypes with individuals from both Upper and Lower Guinean Blocks. According to nuclear genes, there is no geographic structure in *P. tricupsis* that would fit the main biogeographic zones.

According to Genetic Landscape Shape Analysis, there are low genetic distances among pangolins in Odzala-Kokoua NP, only samples from Brazzaville showed greater genetic distances since they have originated from geographically distant areas. We may therefore assume that the pangolins which were found in the villages originated from one area, i.e. the surrounding of the villages and they were not imported from other parts of Congo. On the contrary, the samples from bushmeat markets in the south of Congo probably came from different parts of the country since they were genetically distant from each other.

We were not able to find any interpretable geographic structure among the individuals of *P. tricupsis* in Odzala-Kokoua National Park (OKNP) which means that there is probably no apparent barrier for the gene-flow in the OKNP.

Given the connection of diversification of *P. tricupsis* to Pleistocene climatic oscillations, *P. tricupsis* could be used as model species for studying the rainforest refugia and the influence of the climatic oscillation on African forest species (Gaubert et al. 2016).

In *S. gigantea*, due to the low number of collected samples (n=19), low number of reasonable quality sequences (especially for nuclear genes) and lack of available GeneBank data, we were not able to run most of the analysis which were used in *P. tricupsis*. Also the majority of

samples was collected in the western periphery of the park and therefore the sampling area was not covered evenly.

All the results of phylogeographic analysis can be biased by uncertain origin of the samples. The samples were collected from killed animals which were encountered in villages or at market. These animals have been probably hunted some distance away and then carried to the village/market where the samples were taken afterwards.

For more detailed small-scale population study we should consider using more variable markers, such as microsatellites, which could provide more details about the actual status of pangolin populations in OKNP.

5.2. Samples

Designing the sampling strategies is challenging in the case of pangolins. Collecting scales or pieces of tissues from hunted animals seems to be the easiest and the least costly method although the geographic coordinates are not accurate. Taking samples from living animals would require capturing them and taking pieces of scales, blood, biopsies or buccal swabs. Given the fact that animals are sensitive to stress (also during handling, Van Thai et al. 2010), taking invasive samples from wild animals would be a risky procedure and not an efficient sampling method. Also we were not able to amplify any of the DNA fragments using the DNA extracted from buccal swabs, probably due to contamination or low amount of extracted template DNA.

More samples need to be taken from so that sampling would cover the area more evenly, as mentioned above. In *S. gigantea*, the low number of collected samples can be connected with the decline of its population (hunters therefore encounter it less often) or the fact that hunters do not keep the scales and rather sell them right away since they are valued on the black market more than scales of *P. tricuspis* (Swiacká 2019).

5.3. Use in pangolin conservation

Pangolins are a difficult group for monitoring since they are elusive, mostly nocturnal and live in burrows or treetops, often in inaccessible areas (Ingram et al. 2019b; Willcox et al. 2019). Therefore there is not much known about their population structure and trends in the wild. Due to unmonitored exploitation for meat and traditional medicinal purposes (Boakye et al. 2014), increasing interest of illegal hunters in African pangolins and growing demand on Asian markets (Ingram et al. 2019b), there is urgent need for population assessment, especially in *P. tetradactyla* and *S. gigantea* for which there has not yet been conducted any population study.

Molecular methods using samples from hunted animals can help better understand the pangolin ecology, population structure and dynamics. This may in combination with local scale data acquired from hunters and villagers contribute to pangolin conservation efforts. Our study confirms that *P. tricuspis* contains several geographic lineages that should be treated as conservation units; this should be considered while designing management plans for the species.

Last but not least, understanding the population structure can help fight the illegal trade with these endangered animals since one would be able to track down the geographic origin of seized pangolins or their parts and thus reveal the course of the local and global trafficking routes.

6. Conclusions

We have proved that scale samples from killed pangolins can be used as a source of genomic DNA for population and phylogeographic studies. Analysis of mitochondrial and nuclear data revealed high diversity of populations of both species (*P. tricuspis* and *S. gigantea*) in Congo supported by high number of identified haplotypes in our datasets. We observed separate haplotype group of *P. tricuspis* occurring in Congo and thus the data support cryptic diversity *P. tricuspis* populations across its range.

The effective population species had quite stable course with a population growth in *P. tricuspis* during the Pleistocene and a recent decline in both species caused probably mainly by habitat changes.

We have found low genetic differences among samples of *P. tricuspis* originating from Odzala-Kokoua NP indicating that the pangolins were hunted in the surroundings of the sampled villages. The pangolins from markets in South Congo which showed high genetic distances.

More samples (particularly in *S. gigantea*) or different markers has to be used in order to get more accurate information about pangolin populations in Congo. Nevertheless, the molecular methods in combination with local scale data have proved to be useful tool for conservation management of pangolins (not only) in Congo.

7. References

- Akpona HA, Djagoun CAMS, Sinsin B. 2008. Ecology and ethnozoology of the three-cusped pangolin *Manis tricuspis* (Mammalia, Pholidota) in the Lama forest reserve, Benin. *Mammalia* **72**:198–202.
- Alacs EA, Georges A, FitzSimmons NN, Robertson J. 2010. DNA detective: A review of molecular approaches to wildlife forensics. *Forensic Science, Medicine, and Pathology* **6**:180–194.
- Anthony NM et al. 2007. The role of Pleistocene refugia and rivers in shaping gorilla genetic diversity in central Africa. *Proceedings of the National Academy of Sciences of the United States of America* **104**:20432–20436.
- Arnason U, Adegoke JA, Bodin K, Born EW, Esa YB, Gullberg A, Nilsson M, Short R V., Xu X, Janke A. 2002. Mammalian mitogenomic relationships and the root of the eutherian tree. *Proceedings of the National Academy of Sciences* **99**:8151–8156.
- Bandelt HJ, Forster P, Röhl A. 1999. Median-joining networks for inferring intraspecific phylogenies. *Molecular Biology and Evolution* **16**:37–48.
- Boakye MK, Pietersen DW, Kotzé A, Dalton DL, Jansen R. 2014. Ethnomedicinal use of African pangolins by traditional medical practitioners in Sierra Leone. *Journal of ethnobiology and ethnomedicine* **10**:76.
- Challender D, Willcox DHA, Panjang E, Lim N, Nash H, Heinrich S, Chong J. 2019a. *Manis javanica* (Sunda Pangolin). International Union for Conservation of Nature and Natural Resources. Available from <https://dx.doi.org/10.2305/IUCN.UK.2019-3.RLTS.T12763A123584856.en> (accessed May, 2020).
- Challender D, Wu S, Kaspal P, Khatiwada A, Ghose A, Ching-Min Sun N, Mohapatra RK, Laxmi Suwal T. 2019b. *Manis pentadactyla* (Chinese Pangolin). International Union for Conservation of Nature and Natural Resources. Available from

- <https://dx.doi.org/10.2305/IUCN.UK.2019-3.RLTS.T12764A168392151.en> (accessed May, 2020).
- Challender DWS, Hywood L. 2012. African pangolins. *Traffic Bulletin* **24**:53–55.
- Challender DWS, Waterman C, Baillie JEM. 2014. Scaling up pangolin conservation. IUCN SSC Pangolin Specialist Group Conservation Action Plan:24.
- Choo SWW et al. 2016. Pangolin genomes and the evolution of mammalian scales and immunity. *Genome Research* **26**:1312–1322.
- CITES. 2017. CITES appendices I, II, III. Page 19 in CITES Appendices I, II, III, Switzerland.
- Darriba D, Taboada GL, Doallo R, Posada D. 2012. jModelTest 2: more models, new heuristics and parallel computing. *Nature methods* **9**:772.
- De Beer C. 2013. Insights into the genetics of the ground pangolin (*Smutsia temminckii*) [PhD. Theses]. University of the Free State, South Africa.
- deMenocal PB. 2004. African climate change and faunal evolution during the Pliocene-Pleistocene. *Earth and Planetary Science Letters* **220**:3–24.
- Drummond AJ, Rambaut A. 2007. BEAST: Bayesian evolutionary analysis by sampling trees. *BMC Evolutionary Biology* **7**:214. BioMed Central.
- Du Toit Z. 2014. Population Genetic Structure of the Ground Pangolin based on Mitochondrial Genomes [PhD. Theses]. University of the Free State, South Africa.
- du Toit Z, Dalton DL, du Plessis M, Jansen R, Grobler JP, Kotzé A. 2020. Isolation and characterization of 30 STRs in Temminck's ground pangolin (*Smutsia temminckii*) and potential for cross amplification in other African species. *Journal of Genetics* **99**.
- du Toit Z, du Plessis M, Dalton DL, Jansen R, Paul Grobler J, Kotzé A.

- 2017a. Mitochondrial genomes of African pangolins and insights into evolutionary patterns and phylogeny of the family Manidae. *BMC Genomics* **18**:1–13.
- Du Toit Z, Grobler JP, Kotzé A, Jansen R, Brettschneider H, Dalton DL, Gaubert P, Antunes A. 2014. The complete mitochondrial genome of Temminck's ground pangolin (*Smutsia temminckii*; Smuts, 1832) and phylogenetic position of the Pholidota (Weber, 1904). *Gene* **551**:49–54.
- du Toit Z, Grobler JP, Kotze A, Jansen R, Dalton DL. 2017b. Scale samples from Temminck's ground pangolin (*Smutsia temminckii*): a non-invasive source of DNA. *Conservation Genetics Resources* **9**:1–4. Springer Netherlands.
- ESRI. 2014. ArcGIS Desktop: Release 10. Redlands: Environmental Systems Research Institute.
- Fuchs J, Bowie RCK. 2015. Concordant genetic structure in two species of woodpecker distributed across the primary West African biogeographic barriers. *Molecular Phylogenetics and Evolution* **88**:64–74.
- Gaubert P et al. 2016. Phylogeography of the heavily poached African common pangolin (Pholidota, *Manis tricuspis*) reveals six cryptic lineages as traceable signatures of Pleistocene diversification. *Molecular Ecology* **25**:5975–5993.
- Gaubert P et al. 2018. The Complete Phylogeny of Pangolins: Scaling Up Resources for the Molecular Tracing of the Most Trafficked Mammals on Earth. *Journal of Heredity* **109**:347–359.
- Gaubert P, Antunes A. 2005. Assessing the Taxonomic Status of the Palawan Pangolin *Manis culionensis* (Pholidota) Using Discrete Morphological Characters. *Journal of Mammalogy* **86**:1068–1074.
- Gaubert P, Wible JR, Heighton SP, Gaudin TJ. 2020. Phylogeny and systematics. Pages 25–39 in D. W. S. Challender, H. C. Nash, and C. Waterman, editors. *Pangolins*. Academic Press, Cambridge.
- Gaudin TJ, Emry RJ, Pogue B. 2006. A new genus and species of

- pangolin (Mammalia, Pholidota) from the late Eocene of Inner Mongolia, China. *Journal of Vertebrate Paleontology* **26**:146–159.
- Gaudin TJ, Emry RJ, Wible JR. 2009. The phylogeny of living and extinct pangolins (Mammalia, Pholidota) and associated taxa: A morphology based analysis. *Journal of Mammalian Evolution* **16**:235–305.
- Gudehus M, Pietersen DW, Hoffmann M, Cassidy R, Cassidy T, Sodeinde O, Lapuente J, Assovi BG-M, Shirley MH. 2020. Black-bellied pangolin *Phataginus tetradactyla* (Linnaeus, 1766). Pages 123–138 in D. W. S. Challender, H. C. Nash, and C. Waterman, editors. *Pangolins*. Academic Press, Cambridge.
- Guindon S, Gascuel O. 2003. A simple, fast and accurate method to estimate large phylogenies by maximum-likelihood. *Systematic Biology* **52**: 696-704.
- Hassanin A, Hugot JP, Van Vuuren BJ. 2015. Comparison of mitochondrial genome sequences of pangolins (Mammalia, Pholidota). *Comptes Rendus - Biologies* **338**:260–265.
- Heinrich S, Ross J V., Cassey P. 2019. Of cowboys, fish, and pangolins: US trade in exotic leather. *Conservation Science and Practice* **1**:1–10.
- Heinrich S, Wittman TA, Ross J V, Shepherd CR, Challender DWS, Cassey P. 2017. The Global Trafficking of Pangolin: A comprehensive summary of Seizures and trafficking routes from 2010-2015. *Page Traffic*.
- Heinrich S, Wittmann TA, Prowse TAA, Ross J V., Delean S, Shepherd CR, Cassey P. 2016. Where did all the pangolins go? International CITES trade in pangolin species. *Global Ecology and Conservation* **8**:241–253.
- Hoffmann M et al. 2020. Giant pangolin *Smutsia gigantea* (Illiger, 1815). Pages 157–173 in D. W. S. Challender, H. C. Nash, and C. Waterman, editors. *Pangolins*. Academic Press, Cambridge.
- Hsieh HM, Lee JCI, Wu JH, Chen CA, Chen YJ, Wang GB, Chin SC,

- Wang LC, Linacre A, Tsai LC. 2011. Establishing the pangolin mitochondrial D-loop sequences from the confiscated scales. *Forensic Science International: Genetics* **5**:303–307.
- Huntley JW, Voelker G. 2016. Cryptic diversity in Afro-tropical lowland forests: The systematics and biogeography of the avian genus *Bleda*. *Molecular Phylogenetics and Evolution* **99**:297–308.
- Ichu IG. 2019. Status of Pangolin Trade in Cameroon and between Cameroon and destination countries. TRAFFIC. Yaoundé, Cameroon and Cambridge, UK.
- Ingram D, Shirley M, Pietersen D, Godwill Ichu I, Sodeinde O, Moumbolou C, Hoffmann M, Gudehus M, Challender D. 2019a. *Phataginus tetradactyla* (Black-bellied Pangolin). International Union for Conservation of Nature and Natural Resources. Available from <https://www.iucnredlist.org/species/12766/123586126> (accessed April, 2020).
- Ingram DJ et al. 2018. Assessing Africa-Wide Pangolin Exploitation by Scaling Local Data. *Conservation Letters* **11**:e12389.
- Ingram DJ, Coad L, Scharlemann JPW. 2016. Hunting and sale of pangolins across sub-Saharan Africa: a preliminary analysis. Page Offtake Working Paper No. 1.
- Ingram DJ, Cronin DT, Challender DWS, Venditti DM, Gonder MK. 2019b. Characterising trafficking and trade of pangolins in the Gulf of Guinea. *Global Ecology and Conservation* **17**:e00576.
- IUCN. 2020. The IUCN Red List of Threatened Species. International Union for Conservation of Nature and Natural Resources. Available from <https://www.iucnredlist.org> (accessed February, 2020).
- Jansen R, Sodeinde O, Soewu D, Pietersen DW, Alempijevic D, Ingram DJ. 2020. White-bellied pangolin *Phataginus tricuspis* (Rafinesque, 1820). Pages 139–156 in D. W. S. Challender, H. C. Nash, and C. Waterman, editors. *Pangolins*. Academic Press, Cambridge.
- Jun J, Han SH, Jeong TJ, Park HC, Lee B, Kwak M. 2011. Wildlife forensics using mitochondrial DNA sequences: Species

- identification based on hairs collected in the field and confiscated tanned Felidae leathers. *Genes and Genomics* **33**:721–726.
- Khwaja H et al. 2019. Pangolins in global camera trap data: Implications for ecological monitoring. *Global Ecology and Conservation* **20**:e00769.
- Kingdon J, Happold David, Butynski T, Hoffmann M, Happold M, Kalina J. 2013. *Mammals of Africa*. Page Volume V: Carnivore, Pangolins, Equids and Rhinoceroses. Bloomsbury Publishing, London.
- Kirschel ANG, Slabbekoorn H, Blumstein DT, Cohen RE, Kort SR De, Buermann W, Smith TB. 2011. Testing alternative hypotheses for evolutionary diversification in an african songbird: Rainforest refugia versus ecological gradients. *Evolutionary Diversification in an African Songbird Rainforest Refugia*. *Evolution* **65**:3162–3174.
- Kumar Prakash V et al. 2018. Phylogenetic relationship and molecular dating of Indian pangolin (*Manis crassicaudata*) with other extant pangolin species based on complete cytochrome b mitochondrial gene. *Mitochondrial DNA Part A: DNA Mapping, Sequencing, and Analysis* **29**:1276–1283.
- Kumar VP, Kumar D, Goyal SP. 2014. Wildlife DNA Forensic in Curbing Illegal Wildlife Trade: Specie Identification from Seizures. *International Journal of Forensic Science & Pathology* **2**:38–42.
- Kumar VP, Rajpoot A, Mukesh, Shukla M, Kumar D, Goyal SP. 2016. Illegal trade of Indian Pangolin (*Manis crassicaudata*): Genetic study from scales based on mitochondrial genes. *Egyptian Journal of Forensic Sciences* **6**:524–533.
- Leaché AD, Fujita MK. 2010. Bayesian species delimitation in West African forest geckos (*Hemidactylus fasciatus*). *Proceedings of the Royal Society B: Biological Sciences* **277**:3071–3077.
- Luczon AU, Ong PS, Quilang JP, Fontanilla IKC. 2016. Determining species identity from confiscated pangolin remains using DNA barcoding. *Mitochondrial DNA Part B: Resources* **1**:763–766.
- Luo SJ et al. 2007. Isolation and characterization of microsatellite

- markers in pangolins (Mammalia, Pholidota, *Manis* spp.): Primer note. *Molecular Ecology Notes* **7**:269–272.
- MacDonald DW. 2006. *The Encyclopedia of Mammals*. Oxford University Press, London.
- Mahmood T, Challender D, Khatiwada A, Andleeb S, Perera P, Trageser S, Ghose A, Mohapatra R. 2019. *Manis crassicaudata* (Indian Pangolin). International Union for Conservation of Nature and Natural Resources. Available from <https://dx.doi.org/10.2305/IUCN.UK.2019-3.RLTS.T12761A123583998.en> (accessed May, 2020).
- Mason VC, Helgen KM, Murphy WJ. 2019. Comparative Phylogeography of Forest-Dependent Mammals Reveals Paleo-Forest Corridors throughout Sundaland. *Journal of Heredity* **110**:15–172.
- Miller MP. 2005. Alleles In Space (AIS): Computer software for the joint analysis of interindividual spatial and genetic information. *Journal of Heredity* **96**:722–724.
- Mwale M, Dalton DL, Jansen R, De Bruyn M, Pietersen D, Mokgokong PS, Kotzé A. 2016. Forensic application of DNA barcoding for identification of illegally traded African pangolin scales. *Genome* **60**:272–284.
- Nash HC et al. 2018. Conservation genomics reveals possible illegal trade routes and admixture across pangolin lineages in Southeast Asia. *Conservation Genetics* **19**:1083–1095.
- Naturalis ICT. 2020. Catalogue of Life. Naturalis ICT. Available from <http://www.catalogueoflife.org/> (accessed April, 2020).
- Nichol JE. 1999. Geomorphological Evidence and Pleistocene Refugia in Africa. *The Geographical Journal* **165**:79–89.
- Nicolas V, Missoup AD, Denys C, Kerbis Peterhans J, Katuala P, Couloux A, Colyn M. 2011. The roles of rivers and Pleistocene refugia in shaping genetic diversity in *Praomys misonnei* in tropical Africa. *Journal of Biogeography* **38**:191–207.
- Nixon S, Pietersen D, Challender D, Hoffmann M, Godwill Ichu I, Bruce

- T, Ingram D, Matthews N, Shirley M. 2019. *Smutsia gigantea* (Giant Pangolin). International Union for Conservation of Nature and Natural Resources. Available from <https://www.iucnredlist.org/species/12762/123584478> (accessed April, 2020).
- Ogden R, Dawnay N, McEwing R. 2009. Wildlife DNA forensics - Bridging the gap between conservation genetics and law enforcement. *Endangered Species Research* **9**:179–195.
- Pietersen D, Jansen R, Connelly E. 2019a. *Smutsia temminckii* (Temminck’s Pangolin). International Union for Conservation of Nature and Natural Resources. Available from <https://dx.doi.org/10.2305/IUCN.UK.2019-3.RLTS.T12765A123585768.en>. (accessed May, 2020).
- Pietersen D, Moumbolou C, Ingram D, Soewu D, Jansen R, Sodeinde O, Keboy Mov Linkey Iflankoy C, Challender D, Shirley M. 2019b. *Phataginus tricuspis* (White-bellied Pangolin). International Union for Conservation of Nature and Natural Resources. Available from <https://www.iucnredlist.org/species/12767/123586469> (accessed April, 2020).
- Pietersen DW, Challender DWS. 2020. Research needs for pangolins. Pages 537–543 in D. W. S. Challender, H. C. Nash, and C. Waterman, editors. *Pangolins*. Academic Press, Cambridge.
- Publication Office of the European Union. 2019. Commission Regulation (EU) 2019/2117. Page 320/35 in *Official Journal of the European Union*, Belgium.
- Rambaut A, Drummond AJ, Xie D, Baele G, Suchard MA. 2018. Posterior Summarization in Bayesian Phylogenetics Using Tracer 1.7. *Systematic Biology* **67**:901–904.
- Rowe G, Beebe TJC. 2008. *An introduction to molecular ecology*, 2nd edition. Oxford University Press, New York.
- Rozas J, Ferrer-Mata A, Sanchez-DelBarrio JC, Guirao-Rico S, Librado P, Ramos-Onsins SE, Sanchez-Gracia A. 2017. DnaSP 6: DNA

- sequence polymorphism analysis of large data sets. *Molecular Biology and Evolution* **34**:3299–3302.
- Runge J. 2008. Dynamics of Forest Ecosystems in Central Africa During the Holocene: Past – Present – Future: Palaeoecology of Africa, An International Yearbook of Landscape Evolution and Palaeoenvironments. CRC Press, Yaoundé, Cameroon and Cambridge, UK.
- Schoppe S, Katsis L, Lagrada L. 2019. *Manis culionensis* (Philippine Pangolin). International Union for Conservation of Nature and Natural Resources. Available from <https://dx.doi.org/10.2305/IUCN.UK.2019-3.RLTS.T136497A123586862.en> (accessed May, 2020).
- Sen S. 2013. Dispersal of African mammals in Eurasia during the Cenozoic: Ways and whys. *Geobios* **46**:159–172.
- Species+. 2020. Manidae. Species+. Available from <https://speciesplus.net/species> (accessed April, 2020).
- Stephens M, Scheet P. 2005. Accounting for decay of linkage disequilibrium in haplotype inference and missing-data imputation. *American Journal of Human Genetics* **76**:449–462.
- Stephens M, Smith NJ, Donnelly P. 2001. A new statistical method for haplotype reconstruction from population data. *American Journal of Human Genetics* **68**:978–989.
- Swiacká M. 2019. Market survey and population characteristics of three species of pangolins (Pholidota) in the Republic of the Congo [MSc. Theses]. Czech University of Life Sciences Prague.
- Van Thai N, Clark L, Quang T, Phuong PC, Van Nguyen T, Clark L, Quang PT. 2010. Sunda pangolin *Manis javanica* husbandry guidelines (*Manis javanica*). Carnivore and Pangolin Conservation Program - Save Vietnam's Wildlife, Vietnam.
- Văn Thảo Đ, Văn Thành N, Thúy Hà D, Lê Đức Minh và, Đỗ V, Văn Thành N, Hà T, Lê Đức Minh và. 2006. Genetic Assessment of the Sunda Pangolin (*Manis javanica*) Using Degraded and Fresh

- samples: Project Report. Vietnam National University, Hanoi.
- Wasser SK, Joseph Clark W, Drori O, Stephen Kisamo E, Mailand C, Mutayoba B, Stephens M. 2008. Combating the illegal trade in African elephant ivory with DNA forensics. *Conservation Biology* **22**:1065–1071.
- Willcox D et al. 2019. Evaluating methods for detecting and monitoring pangolin (Pholidata: Manidae) populations. *Global Ecology and Conservation* **17**:e00539.
- Yu HT, Ma GC, Lee DJ, Chin SC, Tsao HS, Wu SH, Shih SY, Chen M. 2011. Molecular delineation of the Y-borne Sry gene in the Formosan pangolin (*Manis pentadactyla pentadactyla*) and its phylogenetic implications for Pholidota in extant mammals. *Theriogenology* **75**:55–64.
- Zhang H, Miller MP, Yang F, Chan HK, Gaubert P, Ades G, Fischer GA. 2015. Molecular tracing of confiscated pangolin scales for conservation and illegal trade monitoring in Southeast Asia. *Global Ecology and Conservation* **4**:414–422.

Appendices

List of the Appendices:

Appendix 1: List of samples villages in Congo and their coordinates.

Appendix 1: List of samples villages in Congo and their coordinates

Village	Latitude	Longitude
Atención	1.309589	15.7910021
Bad	1.608171	14.81680636
Batekock	1.610631	14.75295857
Belvi	1.581560	14.44375274
Bessie	1.620983	14.72720232
Bossouaka	0.477806	14.48407443
Brazzaville	-4.286357	15.25064797
Douma	1.575540	15.23337352
Ebana	0.147433	14.87949866
Egnabi	1.641885	14.64814852
Etoumbi	0.022563	14.89340565
Goa	1.583020	15.10773964
Ketta	1.504889	15.91604113
Kokoua	1.597186	15.4914985
Lango	0.782336	15.31389662
Lango checkpoint	0.768540	15.30088
Lebango	0.388400	14.78712421
Liouesso	1.644150	15.69339355
Makoua	0.003427	15.6266619
Mani	4.326990	12.36466
Mbomandzokou	0.605217	14.39054784
Mbomo	0.433844	14.86431193
Mekoume	1.606454	15.00449142
Mickel	1.682211	14.57828067
Midjandja	1.609943	14.8390761
Midzong	1.570514	14.39987258
Mielekouka	1.568724	15.1764455
Mobangui	0.826165	15.49539574
Mokouandgonda	0.827165	15.46196376
Mouangi	0.461081	14.50268238
Nakoaka	1.649475	14.64269043
Ngo	2.485263	15.741799
Oloba	0.662765	14.36187776
Ouessou	1.608952	16.99990027

Seka	1.568336	15.40460853
Seka Kodou	1.605572	14.79744052
Sembe	1.643972	14.58326827
Tolo	0.538471	14.42934842
Zoulaboth	1.693040	14.53431306